

MBMcNeil

**EPRI**  
Electric Power  
Research Institute

Keywords:  
Pitting  
Corrosion testing  
Corrosion  
Electrochemistry  
Electrochemical potentials

EPRI EAR-7489  
Project 8002-15  
Final Report  
October 1991



## Using Pitting and Protection Potentials to Predict Pitting Behavior: New Insights

Prepared by  
Cortest Columbus Technologies  
Columbus, Ohio

*Legacy-20*

## Using Pitting and Protection Potentials to Predict Pitting Behavior: New Insights

Pitting and protection potentials ( $E_{pit}$  and  $E_{prot}$ ), determined in conventional cyclic potentiodynamic polarization tests, often provide inconsistent assessments of the pitting resistance of stainless alloys. A new parameter,  $E_u$ , falling between  $E_{pit}$  and  $E_{prot}$  values, provides a more practical and consistent assessment of pitting resistance.

---

### INTEREST CATEGORIES

Materials  
Fossil steam plant systems  
and performance  
Nuclear plant corrosion  
control  
Service water systems

---

### KEYWORDS

Pitting  
Corrosion testing  
Corrosion  
Electrochemistry  
Electrochemical potentials

---

**BACKGROUND** In a cyclic potentiodynamic polarization (CPP) test, the potential of a stainless alloy specimen immersed in a corrosive solution is changed at a constant rate to more noble (positive) values until pitting initiates at  $E_{pit}$ ; then the potential is changed to more active (negative) values until the pits repassivate (stop growing) at  $E_{prot}$ . Conventional wisdom states that the more noble the value of  $E_{pit}$  or  $E_{prot}$ , the more resistant the alloy is to pitting.

Unfortunately, the ranking of alloys often depends on whether  $E_{pit}$  or  $E_{prot}$  is chosen as the ranking parameter; the relationship between  $E_{pit}$  and  $E_{prot}$ , if any, is unknown; and the value of each parameter is quite sensitive to experimental procedures. Consequently, design engineers are reluctant to select materials of construction based solely on the results of the CPP test and instead rely more on the results of long-term field tests. These tests unfortunately have their own shortcomings.

---

**OBJECTIVES** To understand the relationship between  $E_{pit}$  and  $E_{prot}$ ; to define a pitting parameter that is not sensitive to experimental procedure and that can be used to provide an accurate ranking of the pitting resistance of alloys.

---

**APPROACH** The project team determined the pitting resistance of Type 317L stainless steel and alloy G3 in several test solutions that simulated flue gas desulfurization system outlet duct environments. CPP tests, performed at two potential sweep rates, provided baseline  $E_{pit}$  and  $E_{prot}$  values. The researchers then held specimens at constant potentials between  $E_{pit}$  and  $E_{prot}$  to determine how pit initiation time varied with potential. Finally, they performed modified ASTM Standard F-746 tests to determine the sensitivity of the  $E_{prot}$  value to previous pit growth. In this test, they held the potential of the specimen at a relatively noble value to stimulate pit growth. After a preselected time of growth, they dropped the potential to a lower value to establish the repassivation potential,  $E_{prot}$ .

---

**RESULTS** The CPP and constant potential tests demonstrated that pitting is a stochastic process resulting in significant scatter of the measured  $E_{pit}$  values. Nevertheless, the results clearly showed that  $E_{pit}$  decreased as the potential sweep rate decreased in CPP tests and as the exposure period increased in constant potential tests. The researchers identified a unique pitting potential ( $E_u$ ), defined as the potential above which the pit nucleation frequency exceeds zero.  $E_u$  corresponds to the most active value of  $E_{pit}$  recorded, associated with long

---

exposure periods. The modified ASTM Standard F-746 tests confirmed that  $E_{\text{prot}}$  decreased as the time of previous pit growth increased. After minimal pit growth, when the environment within the pit is similar to the bulk environment,  $E_{\text{prot}}$  is approximately equal to  $E_u$ .

---

**EPRI PERSPECTIVE**  $E_u$  is a unique pitting potential, falling between the  $E_{\text{pit}}$  and  $E_{\text{prot}}$  values determined in CPP tests.  $E_u$  is not influenced by experimental procedure and, as such, accurately characterizes the long-term pitting resistance of an alloy. Ideally, design engineers should select materials of construction after comparing  $E_u$  values for candidate alloys in the expected service environment. If only CPP test results are available, the more conservative  $E_{\text{prot}}$  value should be used.  $E_{\text{pit}}$  is less conservative (more positive) than  $E_u$  and is not an acceptable basis for predicting long-term pitting performance.

---

#### **PROJECT**

**RP8002-15**

**Project Manager: Barry C. Syrett**

**Office of Exploratory and Applied Research**

**Contractor: Cortest Columbus Technologies**

**For further information on EPRI research programs, call  
EPRI Technical Information Specialists (415) 855-2411.**

# Using Pitting and Protection Potentials to Predict Pitting Behavior: New Insights

EAR-7489  
Research Project 8002-15

Final Report, October 1991

Prepared by  
CORTEST COLUMBUS TECHNOLOGIES  
2704 Sawbury Boulevard  
Columbus, Ohio 43235

## DISCLAIMER OF WARRANTIES AND LIMITATION OF LIABILITIES

THIS REPORT WAS PREPARED BY THE ORGANIZATION(S) NAMED BELOW AS AN ACCOUNT OF WORK SPONSORED OR COSPONSORED BY THE ELECTRIC POWER RESEARCH INSTITUTE, INC. (EPRI). NEITHER EPRI, ANY MEMBER OF EPRI, ANY COSPONSOR, THE ORGANIZATION(S) NAMED BELOW, NOR ANY PERSON ACTING ON BEHALF OF ANY OF THEM:

(A) MAKES ANY WARRANTY OR REPRESENTATION WHATSOEVER, EXPRESS OR IMPLIED, (I) WITH RESPECT TO THE USE OF ANY INFORMATION, APPARATUS, METHOD, PROCESS, OR SIMILAR ITEM DISCLOSED IN THIS REPORT, INCLUDING MERCHANTABILITY AND FITNESS FOR A PARTICULAR PURPOSE, OR (II) THAT SUCH USE DOES NOT INFRINGE ON OR INTERFERE WITH PRIVATELY OWNED RIGHTS, INCLUDING ANY PARTY'S INTELLECTUAL PROPERTY, OR (III) THAT THIS REPORT IS SUITABLE TO ANY PARTICULAR USER'S CIRCUMSTANCE; OR

(B) ASSUMES RESPONSIBILITY FOR ANY DAMAGES OR OTHER LIABILITY WHATSOEVER (INCLUDING ANY CONSEQUENTIAL DAMAGES, EVEN IF EPRI OR ANY EPRI REPRESENTATIVE HAS BEEN ADVISED OF THE POSSIBILITY OF SUCH DAMAGES) RESULTING FROM YOUR SELECTION OR USE OF THIS REPORT OR ANY INFORMATION, APPARATUS, METHOD, PROCESS, OR SIMILAR ITEM DISCLOSED IN THIS REPORT.

ORGANIZATION(S) THAT PREPARED THIS REPORT:  
CORTEST COLUMBUS TECHNOLOGIES



Printed on Recycled Paper

Prepared for  
Electric Power Research Institute  
3412 Hillview Avenue  
Palo Alto, California 94304

EPRI Project Manager  
B. C. Syrett

Office of Exploratory and Applied Research

Electric Power Research Institute and EPRI are registered service marks of Electric Power Research Institute, Inc.

Copyright © 1991 Electric Power Research Institute, Inc. All rights reserved.

#### ORDERING INFORMATION

Requests for copies of this report should be directed to Research Reports Center (RRC), Box 50490, Palo Alto, CA 94303, (415) 965-4081. There is no charge for reports requested by EPRI member utilities and affiliates, U.S. utility associations, U.S. government agencies (federal, state, and local), media, and foreign organizations with which EPRI has an information exchange agreement. On request, RRC will send a catalog of EPRI reports.

## ABSTRACT

---

A literature review was performed to identify test methods that have been used to examine pitting susceptibility of alloys in chloride ( $\text{Cl}^-$ ) containing environments. Several techniques were identified and a critical analysis of the validity of the different electrochemical methods was performed with special attention given to the causes of variations observed in the pitting, or breakdown, potential ( $E_{\text{pit}}$ ) and the protection, or repassivation, potential ( $E_{\text{prot}}$ ). Experiments were performed on Type 317L stainless steel in three solutions containing high levels of  $\text{Cl}^-$  and Alloy G3 in two solutions containing high levels of  $\text{Cl}^-$ . The test solutions were designed to simulate environments present in flue gas desulfurization systems. Cyclic potentiodynamic polarization (CPP) experiments and constant potential-time experiments (up to 60 days) were performed to examine pit initiation and repassivation; and modified ASTM F-746 tests were performed to establish the protection potential as a function of prior pitting history.

Analysis of the data suggests that there exists a unique pitting potential ( $E_u$ ) defined by the stochastic models for pit initiation that equals the most active value of  $E_{\text{pit}}$  (long incubation times) and that equals the most noble  $E_{\text{prot}}$  value (measured following only minimal pit growth).

# CONTENTS

---

Section	Page
<b>Executive Summary</b> .....	<b>ES-1</b>
<b>1 Introduction</b> .....	<b>1-1</b>
<b>2 Review of Methods to Monitor Pit Initiation</b> .....	<b>2-1</b>
Pit Initiation .....	2-1
Electrochemical Methods .....	2-2
Potentiodynamic Polarization .....	2-2
Stepping Potentiostatic Polarization .....	2-2
Constant Potential-Time .....	2-2
Scratch Technique .....	2-3
Pit Propagation Rate (PPR) Curves .....	2-3
Scanning Vibrating Electrode .....	2-4
Electrochemical Impedance Spectroscopy (EIS) .....	2-4
Electrochemical Noise .....	2-4
Artificial Pits .....	2-5
Galvanostaircase Polarization .....	2-5
Microscopic Examination .....	2-5
Ellipsometry .....	2-6
Validity of Electrochemical Methods .....	2-6
<b>3 Cyclic Potentiodynamic Polarization Experiments</b> .....	<b>3-1</b>
Experimental Approach .....	3-1
Results for Type 317L Stainless Steel .....	3-3
Solution E1 .....	3-3
Solution E2 .....	3-5
Solution E3 .....	3-9

Section	Page
Results for Alloy G3 .....	3-11
Solution E4 .....	3-11
Solution E5 .....	3-13
<b>4 Constant Potential-Time Experiments .....</b>	<b>4-1</b>
Experimental Approach .....	4-1
Results for Type 317L Stainless Steel in Solution E3 .....	4-1
Results for Alloy G3 in Solution E4 .....	4-2
<b>5 Modified ASTM F-746 Tests .....</b>	<b>5-1</b>
Experimental Approach .....	5-1
Results for Type 317L Stainless Steel in Solution E3 .....	5-1
Results for Alloy G3 in Solution E4 .....	5-5
<b>6 Discussion .....</b>	<b>6-1</b>
<b>7 Conclusions .....</b>	<b>7-1</b>
<b>References .....</b>	<b>R-1</b>



# LIST OF FIGURES

---

Figure	Page
<b>1-1</b> Schematic of Typical Anodic Cyclic Potentiodynamic Polarization Curves .....	<b>1-2</b>
<b>3-1</b> Schematic Diagram of the Three-Compartment Electrochemical Cell Used for the CPP Experiments .....	<b>3-2</b>
<b>3-2</b> CPP Curve for Type 317L Stainless Steel in Solution E1 With a PTFE Holder/Specimen Interface Performed at a Scan Rate of 0.6V/h .....	<b>3-3</b>
<b>3-3</b> CPP Curve for Type 317L Stainless Steel in Solution E1 With a PTFE Holder/Specimen Interface Performed at a Scan Rate of 0.06V/h .....	<b>3-4</b>
<b>3-4</b> CPP Curves for Type 317L Stainless Steel in Solution E1 With a Vapor/Liquid Interface Performed at a Scan Rate of 0.6V/h .....	<b>3-4</b>
<b>3-5</b> CPP Curves for Type 317L Stainless Steel in Solution E1 With a Vapor/Liquid Interface Performed at a Scan Rate of 0.06V/h .....	<b>3-5</b>
<b>3-6</b> CPP Curve for Type 317L Stainless Steel in Solution E2 With a PTFE Holder/Specimen Interface Performed at a Scan Rate of 0.6V/h .....	<b>3-7</b>
<b>3-7</b> CPP Curve for Type 317L Stainless Steel in Solution E2 With a PTFE Holder/Specimen Interface Performed at a Scan Rate of 0.06V/h .....	<b>3-7</b>
<b>3-8</b> CPP Curves for Type 317L Stainless Steel in Solution E2 With a Vapor/Liquid Interface Performed at a Scan Rate of 0.6V/h .....	<b>3-8</b>
<b>3-9</b> CPP Curves for Type 317L Stainless Steel in Solution E2 With a Vapor/Liquid Interface Performed at a Scan Rate of 0.06V/h .....	<b>3-8</b>
<b>3-10</b> CPP Curve for Type 317L Stainless Steel in Solution E3 With a PTFE Holder/Specimen Interface Performed at a Scan Rate of 0.6V/h .....	<b>3-9</b>
<b>3-11</b> CPP Curve for Type 317L Stainless Steel in Solution E3 With a PTFE Holder/Specimen Interface Performed at a Scan Rate of 0.06V/h .....	<b>3-10</b>
<b>3-12</b> Curves for Type 317L Stainless Steel in Solution E3 With a Vapor/Liquid Interface Performed at a Scan Rate of 0.6V/h .....	<b>3-10</b>
<b>3-13</b> CPP Curves for Type 317L Stainless Steel in Solution E3 With a Vapor/Liquid Interface Performed at a Scan Rate of 0.06V/h .....	<b>3-11</b>
<b>3-14</b> CPP Curves for Alloy G3 in Solution E4 With a PTFE Holder/Specimen Interface Performed at a Scan Rate of 0.6V/h .....	<b>3-12</b>

Figure	Page
<b>3-15</b> CPP Curves for Alloy G3 in Solution E4 With a PTFE Holder/Specimen Interface Performed at a Scan Rate of 0.06V/h .....	3-13
<b>3-16</b> CPP Curves for Alloy G3 In Solution E4 With a Vapor/Liquid Interface Performed at a Scan Rate of 0.6V/h .....	3-14
<b>3-17</b> CPP Curves for Alloy G3 In Solution E4 With a Vapor/Liquid Interface Performed at a Scan Rate of 0.06V/h .....	3-14
<b>3-18</b> CPP Curves for Alloy G3 in Solution E5 With A PTFE Holder/Specimen Interface Performed at a Scan Rate of 0.6V/h .....	3-15
<b>3-19</b> CPP Curves for Alloy G3 in Solution E5 With a PTFE Holder/Specimen Interface Performed at a Scan Rate of 0.06V/h .....	3-15
<b>3-20</b> CPP Curves for Alloy G3 in Solution E5 With a Vapor/Liquid Interface Performed at a Scan Rate of 0.6V/h .....	3-16
<b>3-21</b> CPP Curves for Alloy G3 in Solution E5 With a Vapor/Liquid Interface Performed at a Scan Rate of 0.06V/h .....	3-16
<b>5-1</b> Current-Time Transients for Type 317L in Solution E3 Following Pit Stimulation at 0.6V (SCE) for 2 Seconds (0.03 min) and Polarized to a Potential Near $E_{prot}$ .....	5-2
<b>5-2</b> Current-Time Transients for Type 317L in Solution E3 Following Pit Stimulation at 0.6V (SCE) for 15 Seconds (0.25 min) and Polarized to a Potential Near $E_{prot}$ .....	5-2
<b>5-3</b> Current-Time Transients for Type 317L in Solution E3 Following Pit Stimulation at 0.6V (SCE) for 2 Minutes and Polarized to a Potential Near $E_{prot}$ (Two Curves Shown for Duplicate Tests at 200mV and 150 mV) .....	5-3
<b>5-4</b> Current-Time Transients for Type 317L in Solution E3 Following Pit Stimulation at 0.6V (SCE) for 7 Minutes and Polarized to a Potential Near $E_{prot}$ (Two Curves Shown for Duplicate Tests at 100 mV) .....	5-3
<b>5-5</b> Current-Time Transients for Type 317L in Solution E3 Following Pit Stimulation at 0.6V (SCE) for 25 Minutes and Polarized to a Potential Near $E_{prot}$ .....	5-4
<b>5-6</b> Current-Time Transients for Type 317L in Solution E3 Following Pit Stimulation at 0.6V (SCE) for 40 Minutes and Polarized to a Potential Near $E_{prot}$ .....	5-4
<b>5-7</b> Current-Time Transients for Type 317L in Solution E3 Following Pit Stimulation at 0.6V (SCE) for 100 Minutes and Polarized to a Potential Near $E_{prot}$ .....	5-5
<b>5-8</b> Current-Time Transients for Alloy G3 in Solution E4 Following Pit Stimulation at 0.6V (SCE) for 15 Seconds (0.25 min) and Polarized to a Potential Near $E_{prot}$ .....	5-6
<b>5-9</b> Current-Time Transients for Alloy G3 in Solution E4 Following Pit Stimulation at 0.6V (SCE) for 2 Minutes and Polarized to a Potential Near $E_{prot}$ .....	5-6
<b>5-10</b> Current-Time Transients for Alloy G3 in Solution E4 Following Pit Stimulation at 0.6V (SCE) for 40 Minutes and Polarized to a Potential Near $E_{prot}$ .....	5-7
<b>6-1</b> Potential Versus Time Data for Alloy 317L in Solution E3 for $E_{pit}$ and $E_{prot}$ ( $E_{pit}$ Versus Time to Pit Initiation and $E_{prot}$ Versus Time Permitted to Pit) .....	6-3
<b>6-2</b> Potential Versus Time Data for Alloy G3 in Solution E4 for $E_{pit}$ and $E_{prot}$ ( $E_{pit}$ Versus Time to Pit Initiation and $E_{prot}$ Versus Time Permitted to Pit) .....	6-3

# LIST OF TABLES

---

Table	Page
3-1 Compositions for Solutions Used in the CPP Experiments .....	3-2
3-2 Values for $E_{cor}$ , $E_{pit}$ , and $E_{prot}$ for Type 317L Stainless Steel Measured by CPP Experiments .....	3-6
3-3 Values for $E_{cor}$ , $E_{pit}$ , and $E_{prot}$ for Alloy G3 Measured by CPP Experiments .....	3-12
4-1 Data for Constant Potential-Time Experiments for Type 317L Stainless Steel in Solution E3 .....	4-2
4-2 Data for Constant Potential-Time Experiments for Alloy G3 in Solution E4 .....	4-3
5-1 Values of $E_{prot}$ as a Function of Time of Pitting From the Modified ASTM F-746 Tests .....	5-5
6-1 CPP Test Data Including (i) Relationship Between $E_{pit}$ and Time to Scan From $E_{prot}$ to $E_{pit}$ , and (ii) Relationship Between $E_{prot}$ and Time From Pit Initiation to Repassivation .....	6-2

## EXECUTIVE SUMMARY

---

A literature review was performed to identify test methods that have been used to examine pitting susceptibility of alloys in chloride ( $\text{Cl}^-$ ) containing environments. Several techniques were identified and a critical analysis of the validity of the different electrochemical methods was performed with special attention given to the causes of variations observed in the pitting, or breakdown, potential ( $E_{\text{pit}}$ ) and the protection, or repassivation, potential ( $E_{\text{prot}}$ ). Experiments were performed on Type 317L stainless steel in three solutions containing high levels of  $\text{Cl}^-$  and Alloy G3 in two solutions containing high levels of  $\text{Cl}^-$ . The test solutions were designed to simulate environments present in flue gas desulfurization systems. Cyclic potentiodynamic polarization (CPP) experiments, constant potential-time experiments (up to 60 days), and modified ASTM F-746 Standard tests were performed to examine pit initiation and repassivation.

Significant scatter was observed in  $E_{\text{pit}}$  values but much less scatter was observed in  $E_{\text{prot}}$  values. The extent of the scatter was controlled, in part, by the presence or absence of preferred pitting sites which, in turn, was influenced by the specimen mounting method: in general, when the junction between the specimen and the PTFE holder was fully immersed in the test solution, the propensity to pitting was higher than when this junction was above the liquid level. Pits (but never crevice corrosion) often initiated preferentially at the PTFE holder/specimen junction. In contrast, pits never initiated preferentially at the vapor/liquid specimen interface, i.e. when the PTFE holder/specimen junction was held above the liquid level. The greatest scatter was observed

for Alloy G3 in a pH 6, high-chloride solution. For tests in which there was a vapor/liquid interface at the specimen surface, pitting occurred in only one of three tests; whereas for two tests in which the PTFE holder/specimen junction was immersed, both specimens pitted in this pH 6 solution. This and other results suggested that the interface between the specimen and the PTFE holder specimen was a preferred pit initiation site.

CPP test results for Type 317L stainless steel in a pH 1 solution containing 1% chloride and for Alloy G3 in a pH 6 solution containing 10% chloride were compared with data generated in constant potential-time tests and modified ASTM F-746 tests. For both of these alloy-solution combinations, the value of  $E_{\text{pit}}$  decreased with increasing exposure period in the constant potential-time tests, the most active values corresponding well with the most active values obtained in the CPP tests. The modified ASTM F-746 tests confirmed that  $E_{\text{prot}}$  is a function of prior pitting history; the longer the period of pit growth prior to repassivation, the more active is the  $E_{\text{prot}}$  value.

Analysis of the data suggests that there is a unique pitting potential ( $E_u$ ) defined by the stochastic models of pit initiation as the potential at which the pit nucleation frequency exceeds zero.  $E_u$  is equal to the most active value of  $E_{\text{pit}}$  recorded in CPP tests or constant potential-time tests (associated with slow scan rates or long exposure periods) and is equal to the most noble  $E_{\text{prot}}$  values recorded when pit growth is minimal.

# 1

## INTRODUCTION

---

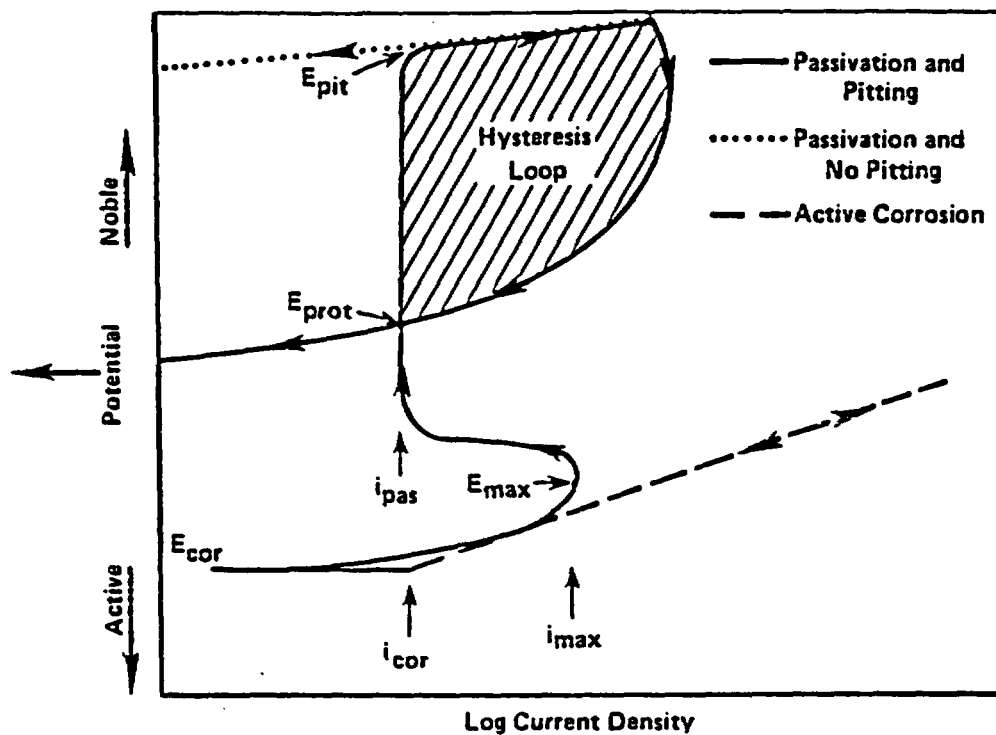
Over the past 20 years, electrochemical tests have been used increasingly to examine the pitting tendencies of alloys. In particular, electrochemical testing has been used extensively to rank alloys with respect to their pitting resistance in a given environment. In addition, electrochemical tests have been used to establish the effects on pitting due to changes in the environment of a given alloy. One of the more popular electrochemical test methods is the cyclic potentiodynamic polarization (CPP) test described in ASTM Standard Practice G61. Schematics of anodic CPP curves illustrating the three primary types of behavior are shown in Figure 1-1. The behavior of interest in this study, passivation and pitting, is given by the solid curve. In the CPP test, two pitting parameters are determined: (1) the pitting, or breakdown, potential ( $E_{pit}$ ), and (2) the protection, or repassivation, potential ( $E_{prot}$ ). It is generally believed that pitting will be initiated very rapidly if the potential of the alloy exceeds  $E_{pit}$ , and that even preexisting pits will repassivate and stop growing if the potential becomes more negative than  $E_{prot}$ .

What happens between  $E_{pit}$  and  $E_{prot}$  is more controversial. It is often claimed that, at potentials between  $E_{pit}$  and  $E_{prot}$ , existing pits may grow, but new pits cannot initiate. However, it is difficult to reconcile this suggestion with the observation that  $E_{pit}$  decreases as the potential scan rate decreases in a CPP test: pits initiate during a slow scan rate test at potentials below the high scan rate  $E_{pit}$  value. Also, it has been claimed that  $E_{prot}$  is the more unique value. However, it has been shown that the degree of pitting prior to reversal of the CPP scan can affect the value of  $E_{prot}$  measured. Amidst this controversy, others claim that electrochemical tests such as the CPP test are of little use in determining the

likelihood of pitting of an alloy in a given environment. Although the relationship between  $E_{pit}$  and  $E_{prot}$  has not been established, it is generally believed that the more positive the values of  $E_{pit}$  and  $E_{prot}$ , the less likely it is that pits will initiate and propagate. Unfortunately, the ranking of alloys often depends on whether  $E_{pit}$  or  $E_{prot}$  is selected as the critical parameter. Thus, the validity of the cyclic potentiodynamic polarization test, as a means of predicting pitting susceptibility, has been questioned.

The primary objective of this work was to determine the time dependency of pit initiation and the prior pitting history dependency on  $E_{prot}$  in an attempt to establish a relationship between  $E_{pit}$  and  $E_{prot}$ . A second objective was to establish the validity of the cyclic potentiodynamic polarization test as a means of predicting pitting susceptibility.

The work to accomplish the above objectives was divided into four tasks: Task 1—Literature Review, Task 2—Cyclic Potentiodynamic Polarization (CPP) Tests, Task 3—Potentiostatic Tests, and Task 4—Modified ASTM F-746 Tests. In Task 1, the existing technical literature was reviewed to establish the present consensus on the validity of electrochemical tests for determining pitting susceptibility, and to identify useful experimental techniques for this study. In Task 2, CPP tests were performed to establish preliminary relationships between  $E_{pit}$ ,  $E_{prot}$ , the corrosion potential ( $E_{cor}$ ), and time. In Task 3, potentiostatic tests were performed to define more precisely the time dependence of pit initiation in the range between  $E_{pit}$  and  $E_{prot}$ . Finally, in Task 4, modified ASTM F-746 tests were performed to establish the effect of prior pitting severity on  $E_{prot}$ .



$E_{cor}$  = corrosion potential

$E_{pit}$  = potential at which pits initiate on forward scan

$E_{prot}$  = potential at which pits repassivate on reverse scan

$E_{Max}$  = potential at active peak

$i_{cor}$  = current density at the free-corrosion potential

$i_{max}$  = current density at active peak

$i_{pas}$  = current density in passive range

Figure 1-1. Schematic of Typical Anodic Cyclic Potentiodynamic Polarization Curves

# 2

## REVIEW OF METHODS TO MONITOR PIT INITIATION

---

Task 1—Literature Review was performed to review the electrochemical methods that have been utilized to examine pitting susceptibility, to establish the validity of these electrochemical test methods, and to identify experimental techniques for accomplishing the objectives of this program. A literature search was performed utilizing the DIALOG computerized search to identify technical articles concerned with pit initiation. The review included Metals and Ceramics Information Center (MCIC), Metadex (Metals Abstracts), 1966–1988, and Chemical Abstracts, 1967–1988. Several papers were reviewed in which a variety of techniques was used to study pit initiation.

### Pit Initiation

The primary goal of this research program was to examine the process of pit initiation and relate it to the parameters of  $E_{\text{pit}}$  and  $E_{\text{prot}}$  as measured by CPP methods. Therefore, a review of the pit initiation process is presented in this section.

Pitting of stainless and nickel-base alloys is a localized form of corrosion that occurs on an otherwise passive, noncorroding surface. Anyone who has studied pitting in the laboratory or examined failures under operating conditions will generally agree that the sites at which pits initiate are randomly oriented on the surface and highly unpredictable. It is true that pitting quite often is associated with specific locations on a given structure, e.g., welds, weld spatter, second phase particles, crevice sites, etc; however, within these preferred locations, pit initiation is random and there are usually areas within the preferred locations without pits. Because of this random nature of pit initiation, stochastic models of pitting

have been developed that attempt to account for the statistical nature of pit initiation.

Williams, Westcott, and Fleischmann reviewed other modeling efforts and presented their own stochastic models of pitting corrosion of stainless steels in two papers.<sup>1, 2</sup> Williams et al.<sup>1</sup> points out that various authors have emphasized various phenomena for pit nucleation including: inhomogeneity in the metal, failure and slow healing of the passive film, development of critical acidity levels in microscopic flaws, defects and their transport in passive films, and chloride absorption or incorporation into localized areas of passive films. An important feature of most of the various models and explanations of pitting is the induction time before pit initiation occurs for a given set of parameters.

The statistical approach presented by Williams et al. views pit nucleation as a rare event that results in current and potential fluctuations randomly distributed in time and space over the metal surface. The model has the following features: (1) nucleation events have a given frequency, (2) these events have a probability of dying, (3) nucleation events that survive beyond a critical age do not die, and (4) each event has an induction time during which the local current does not increase but during which the event may die. Thereby, pits are unstable when they are first nucleated and become stable only after the pit has survived past the critical age.

The particular model proposed by Williams et al.<sup>2</sup> is that the pit nucleation phenomenon is a local acidification caused by local potential and current fluctuations related, in part, to the surface roughness of the specimen and boundary layer in the liquid at the metal surface. Of

most interest to the present study are predictions of the potential dependency of pit initiation. The following conclusions were drawn by Williams et al. First, the nucleation frequency of unstable pits is a function of electrode potential and varies from zero to some limiting value. Thereby, the potential at which the nucleation frequency goes to zero defines a unique critical pitting potential. Second, the death probability of unstable pits is not dependent on electrode potential. Third, the critical age for transition of an unstable to a stable pit and slope of the current-time transients are electrokinetically related properties and are strongly dependent on electrode potential.

### Electrochemical Methods

In any model for pit initiation, the electrode potential is a critical parameter. Furthermore, measurements of current fluctuations due to unstable pit nucleation events and measurements of the significant current increases that follow the initiation of stable pitting are quite easily made utilizing electrochemical methods. Therefore, most of the methods for evaluating pitting corrosion involve electrochemical measurements of electrode potential and current, either while controlling the electrode potential (potentiostatically, potentiodynamically, or a combination of the two), or electrode current (galvanostatically or galvanodynamically), or a combination of the two. The following paragraphs review the various techniques that have been used to evaluate pitting susceptibility.

#### Potentiodynamic Polarization

The CPP test is a method for determining  $E_{pit}$  and  $E_{prot}$  by scanning, at a constant rate, the electrode potential of a specimen while monitoring the corresponding applied current. Figure 1-1 indicates the type of data expected. This is a widely used technique for examining pitting susceptibility. The value of  $E_{pit}$  denotes the potential at which pits initiate on the forward scan and the current increases abruptly. The value of  $E_{prot}$  denotes the potential at which pits are repassivated during the reverse scan, at which point the current decreases back to passive values. The references cited here include studies that examine factors affecting the  $E_{pit}$  and  $E_{prot}$  values or compare data from CPP tests with other electrochemical methods of determining pitting susceptibility. It should be noted that, in several studies, only forward scans were performed<sup>3-10</sup> during the potentiodynamic polarization test. In these tests, only  $E_{pit}$  is available. In

other studies, forward and reverse scans (CPP tests) were performed and both  $E_{pit}$  and  $E_{prot}$  were determined.<sup>11-18</sup> As will be evident in the final discussion section, it is believed that measuring both  $E_{pit}$  and  $E_{prot}$  is critical, especially when making an engineering decision on the susceptibility of a material to pitting corrosion.

One of the arguments against the use of CPP tests for measuring  $E_{pit}$  and  $E_{prot}$  is that neither is a unique value and both are dependent on experimental parameters. It has been shown that the pitting potential becomes more negative with decreasing scan rate.<sup>12, 18</sup> This is easily explained by an incubation process for pitting, in which a slower scan rate permits pit initiation to occur at a more negative potential during the forward CPP scan. The value for  $E_{prot}$  has been shown to be dependent on the presence of crevice attack<sup>12</sup> and on the amount of pitting permitted prior to reversing the potential scan direction.<sup>17, 18</sup> Nader-Roux et al.<sup>12</sup> showed that, when crevice corrosion was present,  $E_{prot}$  was as much as 200mV more negative than when the test specimen was free of crevices. Wilde and Williams<sup>18</sup> showed that the more pitting permitted prior to reversal of the potential scan, the more negative  $E_{prot}$ .

#### Stepping Potentiostatic Polarization

Stepping potentiostatic polarization is a method of producing a polarization curve using discrete potential steps, usually 25–50mV each, as opposed to a constant potential scan as used in a CPP test. Because a fixed time period is maintained between each step, an average rate of potential increase in mV/sec can be calculated. For comparable average scan rates, Zucchi et al.<sup>3</sup> found that similar  $E_{pit}$  values were obtained by CPP and stepping potentiostatic polarization tests.

Williams and Westcott<sup>19</sup> combined a potentiodynamic scanning method with potentiostatic holding of the potential for a specified time while monitoring the current to determine  $E_{pit}$ . This method was further used to help define nucleation frequency data required for modeling efforts.<sup>2, 19</sup>

#### Constant Potential-Time

Several studies have used constant potential, potentiostatic polarization, and monitored current as a function of time to examine the incubation time for pit initiation.<sup>1,2,4,9,13,16,19-21</sup> Important variables of this method typically include the electrode potential, the length of



time of the test, passivation treatment prior to testing, and method of monitoring current. In some of these studies, current fluctuations with time were examined, i.e., pit nucleation events.<sup>1,2,4,19,20</sup> In other studies, the potential for pit initiation was determined when a net current increase was observed.<sup>13,16,21</sup>

Broli and Holtan<sup>21</sup> found that, for aluminum in 3% NaCl solution, the time to pit initiation increased as the electrode potential decreased, but the lowest value of  $E_{\text{pit}}$  measured by a constant potential-time method in 17 hour tests was approximately equal to  $E_{\text{prot}}$  measured with the CPP method. This conclusion was different from work performed by these authors for stainless steel in which  $E_{\text{pit}}$  measured in 83 hour constant potential-time tests remained more positive than the value of  $E_{\text{prot}}$  from CPP tests. A question remains as to whether longer time periods for the potentiostatic tests for the stainless steel would result in  $E_{\text{pit}}$  equal to  $E_{\text{prot}}$  for stainless steels.

### Scratch Technique

In the scratch technique,<sup>3,5,9</sup> a specimen is potentiostatically controlled while monitoring the current. The specimen is scratched with some hard inert material (silicon carbide or glass) to break the passive film, and the current transient is recorded. If the current decreases and the scratched area repassivates, the control potential is more negative than a "pitting potential." If the current continues to increase following the initial current spike, the control potential is more positive than a "pitting potential." By performing the scratch test at a series of potentials, 10 to 50mV apart, the value of a "pitting potential" can be estimated. In a study by Zucchi et al.<sup>3</sup> for Type 304 stainless steel in a 0.1M NaCl solution, the values of the pitting potential determined by stepping potentiostatic polarization (50mV steps every hour) and for the scratch technique were similar. However, with inhibitor added, the  $E_{\text{pit}}$  from the scratch technique showed no change while  $E_{\text{pit}}$  from the stepping potentiostatic polarization method became much more positive. It is the opinion of the author of this report that the scratch technique mechanically removes the inhibiting film and, therefore, the data from the scratch technique do not represent the effects of the inhibitor. These data appear to indicate a severe limitation of the scratch technique in evaluating inhibitors unless a wear process is a part of the intended application.

In a study by Manning et al.,<sup>5</sup> CPP tests (scan rate of 100mV/hr), constant potential-time exposures (170 hours at each potential), and the scratch technique gave similar values for  $E_{\text{pit}}$  for a duplex stainless steel in a pH 4 1N NaCl solution. For a single-phase alloy, the constant potential-time method indicated an  $E_{\text{pit}}$  value that was approximately 160 mV more negative than for the CPP test or the scratch technique. The difference in the findings for the two alloy systems could likely be due to the nucleation event frequency being much greater on the duplex stainless steel as a result of the inhomogeneities caused by the microstructure. Therefore, the single-phase alloy had a longer incubation time than the duplex alloy at any given potential and this showed up in the potentiostatic tests as a more negative value of  $E_{\text{pit}}$  than in the CPP or scratch test. It is clear from these data that of the three techniques evaluated, the long-term constant potential-time experiments proved the best value of the pitting potential.

Although the above discussion indicates reasonably good agreement between the scratch technique and other methods, care should be taken when applying the technique to systems where the mechanical damage affects the pitting process, as was shown for inhibitor testing. The problem with the scratch technique is that the surface is mechanically deformed to expose bare metal as opposed to a natural film breakdown by an aggressive environment. Therefore, relating the passivation/repassivation characteristics of a scratch to an active pit does not appear to be, in general, an analogous situation.

In defense of the scratch technique, the scratching process produces a relatively high current spike. If the pit nucleation process is one of local acidification produced by current fluctuations,<sup>2</sup> the pit nucleation frequency could be greatly increased during the scratching process, thereby promoting pit initiation if the electrode potential is otherwise favorable. However, there remains an incubation time factor that is greatly dependent on the experimental procedure.

### Pit Propagation Rate (PPR) Curves

In the PPR test,<sup>17,22</sup> the following procedure is used: (1) the specimen is scanned (36V/h) to a potential between  $E_{\text{prot}}$  and  $E_{\text{pit}}$  and held at this potential for 10 minutes to establish the baseline value of  $i_{\text{pas}}$  before pitting has initiated, (2) the potential is scanned (36V/h) beyond

$E_{pit}$  until the nominal current density is equal to 100 A/m<sup>2</sup>, (3) the potential is decreased in a single step to a selected potential below  $E_{pit}$  and the current ( $i_{pit}$ ) is monitored for 10 minutes. By subtracting  $i_{pas}$  from  $i_{pit}$  and dividing by the surface area of the pits, average pit growth rates can be calculated as a function of potential.  $E_{prot}$  is defined as the potential at which the pit propagation rate is zero. Syrett showed that  $E_{prot}$  from CPP tests were more negative than  $E_{prot}$  from PPR tests for stainless steels in chloride environments.<sup>17</sup> It is speculated that the more extensive pitting that occurred prior to repassivation in the CPP tests led to the development of a lower-pH, more aggressive environment within the pits. The value of  $E_{prot}$  measured by the PPR method may be less conservative than  $E_{prot}$  measured by the CPP test, but may be a better indication of long-term pit initiation behavior under normal service conditions. The PPR test became the basis of an ASTM standard procedure for determining pitting and crevice corrosion resistance of stainless steels (ASTM Standard F-746). The advantage of the PPR method for determining  $E_{prot}$  is that it provides for a minimum, reproducible amount of pitting prior to evaluating the repassivation (or pit propagating) characteristic of a material.

A very similar technique, referred to as the stationary potentiokinetic method<sup>11</sup> and also as the quasistationary anodic polarization method,<sup>16</sup> utilizes a stepping procedure similar to the PPR test. However, procedures are included to determine both  $E_{prot}$  (similar to PPR test) and  $E_{pit}$ . Once  $E_{prot}$  is determined,  $E_{pit}$  is determined by the following procedure: (1) the specimen is passivated for 10 minutes, (2) the potential is alternated every 15 minutes between (i) a potential 0.025V positive to  $E_{prot}$  and (ii) a potential that is increased in 0.025mV steps to more positive potentials than  $E_{prot}$ .  $E_{pit}$  is the potential at which the current begins to increase and continues to be high when returned to the potential in (i) 0.025V positive to  $E_{prot}$ . Though  $E_{pit}$  measured this way is always more noble than  $E_{prot}$ , this does not preclude the possibility of pit initiation at or close to  $E_{prot}$  if exposure periods were increased far beyond the standard 15 minutes.

### Scanning Vibrating Electrode

The scanning vibrating electrode method, as described by Ishikawa and Isaacs,<sup>23</sup> utilizes a vibrating electrode to develop a three-dimensional plot of the current density profile of a pitting surface. The electrode vibrator assembly vibrates a platinum electrode perpendicular to the specimen surface. A mechanical stage scans in the

X-Y direction. The potential gradients generated in the solution during localized corrosion are measured as the differences in the potential measured at the two extremes of vibration of the electrode. The scanning vibrating electrode method provides a surface map for the current distribution on a specimen surface. By doing so, pit initiation and growth can be monitored. This is an excellent technique for mapping the spacial distribution of pits and for examining the growth and repassivation of pits.

The primary drawbacks are the time and cost associated with the method. Also, continuous information is not available since a finite measurement time is required for mapping the surface. However, the size of the specimen may be decreased to overcome measurement time as a significant drawback as long as the smaller specimen still contains a representative number of pit initiation sites. To establish incubation time at a constant potential would require continuous scanning, one scan after another, until pitting occurred.

### Electrochemical Impedance Spectroscopy (EIS)

EIS is a technique that applies a small amplitude (5–20mV peak-to-peak) AC potential signal to a specimen and simultaneously measures the current response to establish the impedance as a function of frequency in a range typically between 10,000Hz and 0.01Hz. From the impedance as a function of frequency, electrical analog models of the electrochemical surface can be developed that describe the data. Dawson and Ferreira<sup>15,24</sup> have shown that EIS can be used to differentiate between pitting and passive conditions. Although EIS indicated differences between the initiation and propagation stages, EIS is not seen as a viable means to study the onset of pit initiation and incubation time. The same objections apply to EIS as applied to the scanning vibrating electrode method: (1) noncontinuous measurement, and (2) intensive analysis and labor requirements. The EIS technique is viewed more as a tool to examine the mechanism of pitting rather than a means to establish  $E_{pit}$  and  $E_{prot}$ .

### Electrochemical Noise

The electrochemical noise technique has been shown to be quite sensitive in detecting the onset of pit initiation. The concept is simple; prior to the initiation of stable pitting, there is a time in which nucleation events are recorded as current or potential fluctuations. Thereby,

pitting is usually preceded by an increase, or change, in electrochemical noise. These data can be recorded in a relatively simple means by a strip chart recorder or data acquisition system and interpreted by measuring the frequency of large current fluctuations.<sup>1,2,4</sup> Alternatingly, more sophisticated equipment, e.g., ultralow noise potentiostat, a high level of shielding, etc., can be used in conjunction with spectral analysis for data interpretation.<sup>24,25</sup> These techniques are invaluable for more mechanistic studies and model development where estimation of nucleation event frequencies are critical. Also, these techniques are important for the development of monitoring techniques in which the onset of pitting (high rate of nucleation events) could foretell pit initiation and provide an early warning prior to the development of a significant problem.

### Artificial Pits

Artificial pits have been used to study both pit initiation and pit growth. Suzuki and Kitamura used a simulated pit to examine characteristic pitting potentials.<sup>26</sup> In this study, a simulated pit consisting of an occluded anode (as the pit) coupled to a cathodic surface was used. The pitting potential discussed was the critical potential for pit growth or propagation ( $E_p$ ). It should be noted that the potentials measured are potentials using a Luggin capillary probe inserted into the artificial pit, such that IR-drop down the pit is eliminated. One of the conclusions is that "there exists the critical potential for growth of localized corrosion, below which the already initiated localized corrosion can repassivate. This potential can be measured only in an artificial specimen having a local anode insulated from a cathode." Although artificial pits may be reasonable for examining the pitting and repassivation process from a fundamental point of view, there are obvious drawbacks when predicting pitting susceptibility for an industrial application. Primarily, it is difficult to reproduce the localized environment within a pit and/or to verify whether it has been reproduced while using a macro specimen and occluded cell. Thereby, the data would always be suspect.

### Galvanostaircase Polarization

Cyclic galvanostaircase polarization (GSCP) is a test method designed to determine the relative susceptibility of an alloy (especially aluminum alloys) to localized corrosion (pitting and crevice corrosion). In the galvanostaircase method, a current staircase stepping sequence is applied galvanostatically to the working

electrode and the resulting potential transients are recorded. The current steps are increased at some defined average scan rate. Following breakdown, the scan is reversed. The steady-state potentials at the end of the "up-steps" are extrapolated to zero time, or current, to obtain  $E_{pit}$ ; and the steady-state potentials at the end of the "down-steps" are extrapolated to zero current to obtain  $E_{prot}$ . This current-controlled polarization technique has been shown to predict reproducible protection potentials of aluminum alloys where other potential-controlled electrochemical techniques have failed. Other researchers have used the technique for type 304L stainless steels with good correlation to constant-potential corrosion tests. One key advantage of the GSCP technique over potentiostatic techniques (scratch potentiostatic and constant potential techniques) is that it requires much shorter test times and is easier to perform. Both the pitting and protection potentials may be obtained by the technique. Another advantage of the technique is that the total charge passed during the test is precisely controlled and kept to a minimum, thereby allowing corrosion to initiate only at the most susceptible sites.<sup>31</sup>

### Microscopic Examination

Microscopic examination of the specimen surface may be a good way to observe pit initiation and the spacial distribution of pits. However, it is difficult to distinguish propagating pits from passivated pits. Also, the monitoring scheme for viewing the surface to establish incubation time may be complicated. A video camera may be the best way to monitor the surface. Beck<sup>32</sup> used a horizontally mounted specimen in which a glass window was present in the test cell directly across from the 304 stainless steel specimen surface to permit microscopic examination of the pit. Various methods of producing a single pit were attempted. The most successful was the use of lacquer applied to the surface and using a sewing needle tip to create a hole in the lacquer.

As discussed above, the primary problem with this technique is viewing the area in which pitting initiates. Beck eliminated that problem by providing only an extremely small area available for pitting. This method may be appropriate for pit propagation studies; but, for pit initiation, a larger surface is desired to accommodate the statistical nature of pit initiation. Also, microscopic viewing of a specimen is not likely to be as sensitive as electrochemical techniques to the early stages of pit initiation.

### Ellipsometry

Ellipsometry is a technique used to measure the optical properties of a film, from which thickness data can be derived. Sugimoto et al.<sup>33</sup> present data for an 18-8 stainless steel in a NaCl solution using a microscopic ellipsometer that provides a magnification of 600 times. This equipment provided the determination of the thickness and optical constant of the passive film on an area 10 $\mu$ m in diameter. By scanning the specimen surface, the spatial distribution of film thickness within each grain was observed prior to pit initiation. The specimen was potentiostatically controlled and the film thickness was re-measured following pit initiation. It was shown that pits initiated at thin spots in the passive film.

Ellipsometry belongs in the same category as EIS and scanning vibrating electrode methods, i.e., the technique is labor intensive and does not permit continuous measurements.

### Validity of Electrochemical Methods

Arguments against the use of CPP tests for determining pitting susceptibility have centered around  $E_{\text{pit}}$  and  $E_{\text{prot}}$  not being unique values. These arguments do not disqualify the use of CPP tests for determining  $E_{\text{pit}}$  and  $E_{\text{prot}}$ , but merely establish limitations in the interpretation of the CPP data. It is clear that  $E_{\text{pit}}$  measured utilizing a slow scan rate is a nearer steady-state value than  $E_{\text{pit}}$  measured at a fast scan rate since the slow scan rate permits a longer incubation time for pit initiation. In regard to the stochastic model for pit initiation, a value of  $E_{\text{pit}}$  measured by CPP tests is expected to be more positive than a unique value of the critical pitting potential defined as the potential at which the frequency of pit nucleation events goes to zero. Therefore,  $E_{\text{pit}}$  by CPP techniques is a "nonconservative" estimate of the unique critical pitting potential defined by stochastic models. Furthermore, the relationship between  $E_{\text{pit}}$  by CPP and the unique pitting potential have not been established.

The relationship between  $E_{\text{prot}}$  and a unique value of critical pitting potential is even more unclear than for  $E_{\text{pit}}$ . Suzuki and Kitamura<sup>26</sup> define  $E_{\text{prot}}$  as equal to the steady-state potential within the pit with no anodic polarization applied. Thereby, on the reverse potentiodynamic scan, as the potential becomes more negative, the potential difference between the polarized outside surface and the potential within the pit decreases.  $E_{\text{prot}}$  is

the potential at which the potential on the outside surface is the same as the potential within the pit. As the potential of the outside surface is decreased further, the potential within the pit is more positive and a cathodic current will begin to flow into the pit, tending to increase pH and stop pitting.

It is expected that  $E_{\text{prot}}$  provides a conservative value for establishing pitting susceptibility since it is expected that a unique critical pitting potential will be more positive than  $E_{\text{prot}}$ . The more severe the pitting prior to measuring  $E_{\text{prot}}$ , the more negative the value of  $E_{\text{prot}}$  would be.<sup>18</sup> It is not unreasonable to speculate that the above definition of  $E_{\text{prot}}$  would apply to the unique critical pitting potential for which the nucleation frequency goes to zero.

One possible means of removing the variation in  $E_{\text{prot}}$  is to permit significant pitting to occur prior to reversing the potential scan in a CPP test. A more severe pitting environment within the pit will have been permitted to form and the pH will likely correspond to a limiting value for the hydrolysis reactions according to the chemical composition of the alloy being tested. In this manner, a more consistent  $E_{\text{prot}}$  will be measured and one that also is likely to be the most negative value possible. Thereby, a conservative limit for pit repassivation can be obtained, which is desirable from an engineering viewpoint.

From an opposite viewpoint, the PPR technique<sup>17</sup> minimizes the amount of pitting prior to potentiostatic exposure, and it is claimed that a more consistent measurement is made. It is quite possible that, by approaching either limit (gross pitting prior to measuring  $E_{\text{prot}}$  [CPP test] or minimum pitting prior to measuring  $E_{\text{prot}}$  [PPR test]), consistent results can be obtained.

The above considerations do not limit the applicability of electrochemical methods nor do they indicate that electrochemical methods are not valid for establishing  $E_{\text{pit}}$  and  $E_{\text{prot}}$ . Once the causes of variations in  $E_{\text{pit}}$  and  $E_{\text{prot}}$  produced by experimental procedures are realized, proper interpretation of these pitting parameters can be made.

Another criticism of CPP tests is that a great deal of significance is placed in a single test where the process being examined is admittedly of a statistical nature. This is a valid argument for  $E_{\text{pit}}$  and is probably why a

significant variation in the reproducibility of  $E_{\text{pit}}$  data is observed. Fratesi<sup>10</sup> uses a statistical treatment of  $E_{\text{pit}}$  when examining type 316L stainless steel in 3.5% NaCl solution.  $E_{\text{prot}}$ , on the other hand, is not viewed as a statistical-related parameter. Once pits have been initiated, repassivation of the pit is not necessarily related to a statistical model. However, because a range of pit sizes and densities can occur due to the statistical nature of the pit initiation process,  $E_{\text{prot}}$  would be expected to have some

degree of scatter that always lends itself to statistical approaches for presenting data. Therefore, a single CPP experiment is viewed as a valid test for establishing  $E_{\text{prot}}$ . However, it is the author's opinion that any critical experiment in making engineering decisions should be, at a minimum, duplicated or some other statistical approach used (e.g., statistical experimental design and analysis).<sup>34</sup>

# 3

## CYCLIC POTENTIODYNAMIC POLARIZATION EXPERIMENTS

---

The purpose of these experiments was to establish  $E_{pit}$  and  $E_{prot}$  for type 317L stainless steel and Alloy G3 in high-chloride ( $Cl^-$ ) environments as a function of scan rate. CPP experiments were performed in three solutions for Type 317L and two solutions for Alloy G3. The solutions were selected to simulate environments present in flue gas desulfurization (FGD) systems. Since the accuracy of simulation was not a prime objective of this study, some modifications were made to the FGD environments to simplify their preparation. For instance, dissolved oxygen was purged from the solutions rather than added in controlled amounts. Table 3-1 presents the compositions of the solutions used in this study.

### Experimental Approach

The test procedures followed those outlined in ASTM G61-78 "Conducting Cyclic Potentiodynamic Polarization Measurements for Localized Corrosion" with the following exceptions: (1) the test specimen remained in the solution at the test temperature overnight (~20 hours) prior to performing the CPP test; (2) the scan was begun at a potential 50–100mV more negative than the free-corrosion potential; and (3) two scan rates were used: 0.6V/h (the ASTM standard) and 0.06V/h. The purpose of the slow scan was to permit examination of the effect of scan rate on  $E_{pit}$ . The CPP tests were performed using a Santron computer-controlled potentiostat. A platinum wire counter electrode was used and

the potential was controlled with respect to a saturated calomel reference electrode (SCE). Tests were performed in a three-compartment electrochemical cell with the working electrode compartment heated by circulating water through an outside water jacket (see Figure 3-1).

The working electrode was a cylindrical specimen drilled and tapped to permit mounting on to a specimen holder. A significant effort was made to remove the PTFE holder/specimen interface as an initiation site for pitting. The most successful procedure consisted of the following: (1) the specimen was mounted as tightly as possible; (2) the specimen and holder assembly were mounted in a lathe and machined to make a very smooth transition between the PTFE holder and the specimen; and (3) the specimen surface, including the PTFE holder/specimen interface, was ground to a 600-grit finish. Smearing the relatively soft PTFE over the specimen surface was avoided by polishing only from the metal to the PTFE with fresh polishing paper. Some tests were performed using specimens with this PTFE holder/specimen interface; in other tests, this interface was eliminated by using a long specimen that extended out of the solution, which produced a vapor/liquid interface on the specimen surface instead. For the alloy-solution combinations tested, enhanced pitting did not occur at the vapor/liquid interface, while the PTFE holder/specimen interface provided preferred pit initiation sites in several cases.

Table 3-1  
Compositions for Solutions Used in the CPP Experiments

Solution Variables Element*	Test Solution				
	E1	E2	E3	E4	E5
Al ( $\text{Al}_2(\text{SO}_4)_3$ ), mg/L	1	270	10,000	4	20,000
Mg ( $\text{MgSO}_4$ ), mg/L	5,000	5,000	500	5,000	5,000
Cr ( $\text{CrCl}_3$ ), mg/L	1	5	0	0	0
Cu ( $\text{CuCl}_2$ ), mg/L	1	0.2	0	0	0
Fe ( $\text{FeCl}_3$ ), mg/L	1	1	0	0	0
Mo ( $\text{MoO}_3$ ), mg/L	200	200	0	0	0
N ( $\text{NaNO}_3$ ), mg/L	200	1	0	1	1
Cl ( $\text{NaCl}$ ), mg/L	10,000	100,000	10,000	100,000	100,000
Br ( $\text{NaBr}$ ), mg/L	0	0	0	1	500
$\text{O}_2$ ,**	0	0	0	8	0
Temperature, C	50	50	50	50	90
pH (adjusted with $\text{H}_2\text{SO}_4$ )	1.0	6.0	1.0	6.0	1.0

\* Species added as compound given in parentheses.

\*\* Volume percent in cover gas.

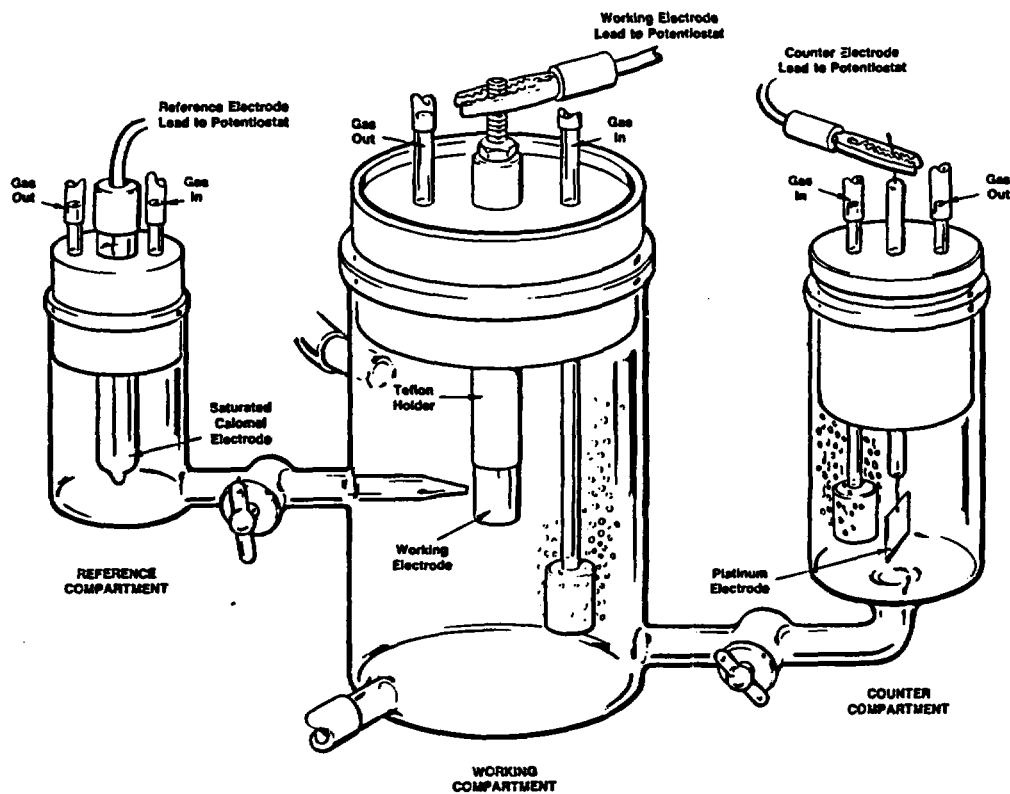


Figure 3-1. Schematic Diagram of the Three-Compartment Electrochemical Cell Used for the CPP Experiments

## Results for Type 317L Stainless Steel

Type 317L stainless steel was tested in three solutions: E1, E2, and E3. For each solution, CPP curves were performed for four conditions: specimens with a PTFE holder/specimen interface at scan rates of 0.6V/h and 0.06V/h, and specimens with a vapor/liquid interface at scan rates of 0.6V/h and 0.06V/h.

### Solution E1

Figures 3-2 to 3-5 show the CPP curves for 317L in Solution E1 for the four conditions described above. Figure 3-2 shows the CPP curve for 317L in Solution E1 with a PTFE holder/specimen interface and performed at a scan rate of 0.6V/h. Pitting occurred on the bulk specimen surface and no enhanced pitting occurred at the PTFE holder/specimen interface. Significant spikes were observed starting at 0.7V, SCE on the forward scan, but stable pitting did not initiate until the reverse scan reached about 0.7V (SCE) as evidenced by the sharp increase in current. The hysteresis observed was quite large with  $E_{prot}$  approximately equal to  $E_{cor}$  Table 3-2

presents  $E_{cor}$ ,  $E_{pit}$ ,  $E_{prot}$ , and a location of attack for each Type 317L specimen tested in Solutions E1, E2, and E3.

Figure 3-3 shows the CPP curve for 317L in Solution E1 with a PTFE holder/specimen interface and performed at a scan rate of 0.06V/h. Pitting was significantly enhanced at the PTFE holder/specimen interface when compared to the remainder of the surface. Comparing the CPP curve in Figure 3-3 to that in Figure 3-2 indicates that  $E_{pit}$  for the slower scan rate (0.06V/h) test was significantly more negative than for the faster scan rate (0.6V/h) test. Because of the presence of enhanced interfacial pitting in the slow scan rate test, it is impossible to say whether the more negative  $E_{pit}$  is due to the lower scan rate or to the preferred pitting sites created by the PTFE holder/specimen interface, or both. Both are expected to make  $E_{pit}$  more negative.

Figure 3-4 shows the CPP curves for duplicate 317L specimens in Solution E1 with a vapor/liquid interface and performed at a scan rate of 0.6V/h. The data for the duplicate specimens indicate approximately 70mV

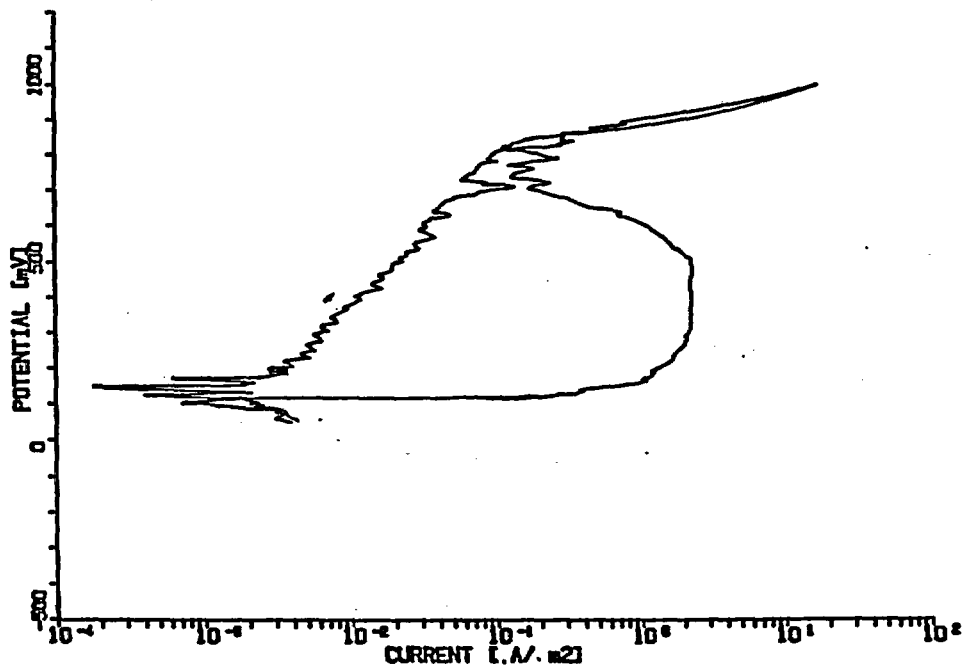


Figure 3-2. CPP Curve for Type 317L Stainless Steel In Solution E1 With a PTFE Holder/Specimen Interface Performed at a Scan Rate of 0.6V/h



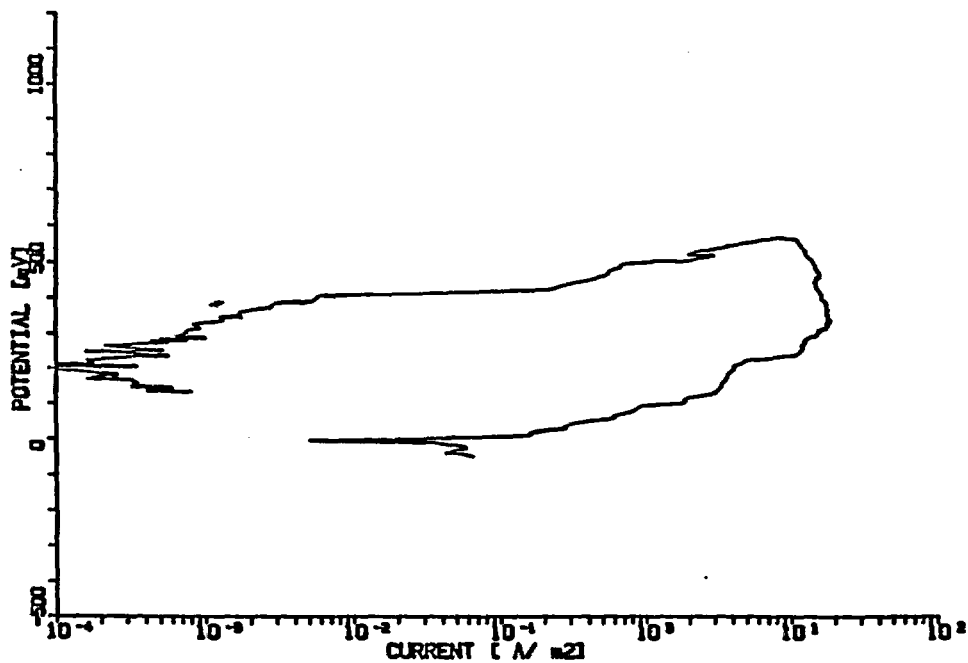


Figure 3-3. CPP Curve for Type 317L Stainless Steel in Solution E1 With a PTFE Holder/Specimen Interface Performed at a Scan Rate of 0.06V/h

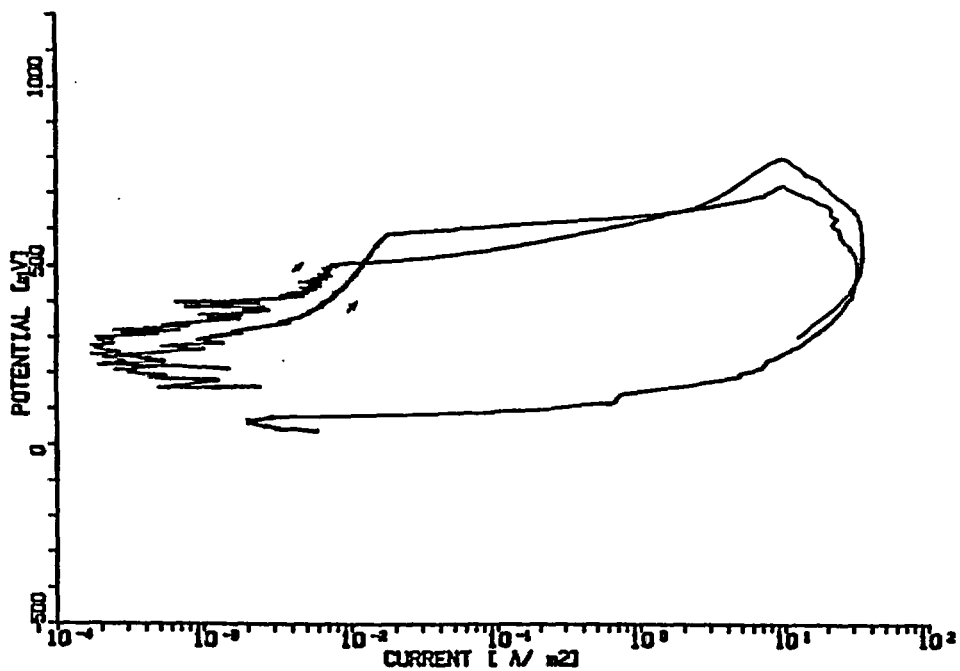


Figure 3-4. CPP Curves for Type 317L Stainless Steel in Solution E1 With a Vapor/Liquid Interface Performed at a Scan Rate of 0.6V/h

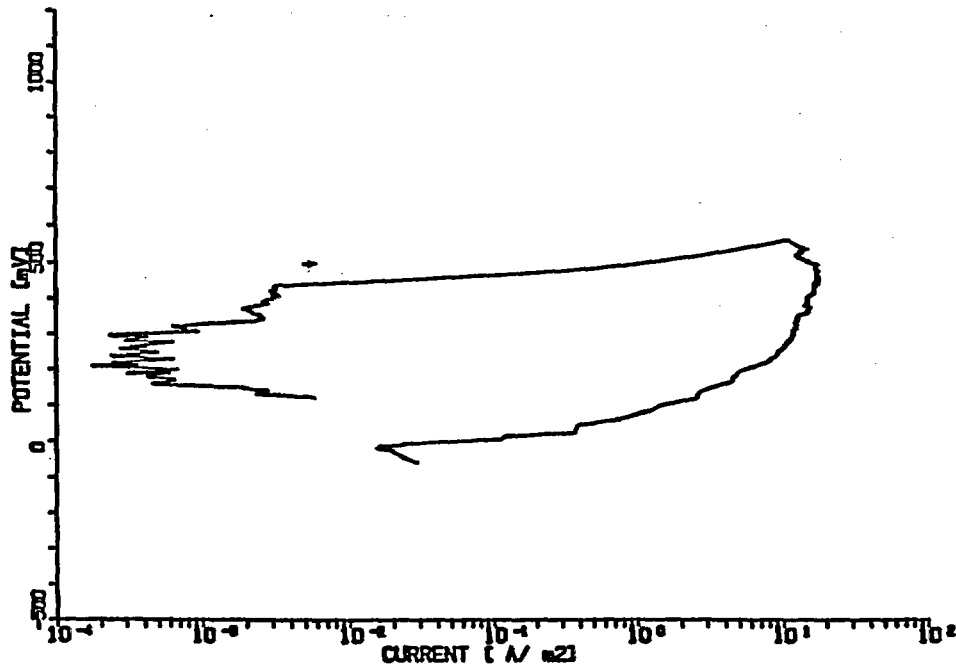


Figure 3-5. CPP Curves for Type 317L Stainless Steel In Solution E1 With a Vapor/Liquid Interface Performed at a Scan Rate of 0.06V/h

difference in  $E_{pit}$ . A comparison of  $E_{prot}$  is not available because one test was inadvertently interrupted before the return scan was complete. No enhanced pitting was ever observed at the vapor/liquid interface. Comparison of the CPP curves in Figure 3-4 (vapor/liquid interface: 0.6V/h) to Figure 3-2 (PTFE holder/specimen interface: 0.6V/h) indicates that  $E_{pit}$  is significantly more negative when the vapor/liquid interface was present than when the PTFE holder/specimen interface was present. This is somewhat unexpected and is not typical of results for other alloy-solution combinations. Values of  $E_{prot}$  for the two conditions discussed above (vapor/liquid versus PTFE holder/specimen interface at 0.6V/h) are within approximately 50mV.

Figure 3-5 shows the CPP curve for 317L in Solution E1 with a vapor/liquid interface and performed at a scan rate of 0.06V/h. Comparison of the CPP curve shown in

Figure 3-5 with the curve shown in Figure 3-4, performed at a faster scan rate, indicates both  $E_{pit}$  and  $E_{prot}$  are somewhat more negative for the slower scan rate. Comparison of the CPP curve in Figure 3-5 (vapor/liquid interface: 0.06V/h) to that shown in Figure 3-3 (PTFE holder/specimen interface: 0.06V/h) shows that the two curves are nearly identical. Values of  $E_{pit}$  are within 50mV and values of  $E_{prot}$  are within 20mV.

#### Solution E2

Figure 3-6 shows the CPP curve for 317L in Solution E2 with a PTFE holder/specimen interface and performed at a scan rate of 0.6V/h. Very little, if any, preferential pitting was associated with the PTFE holder/specimen interface. Pitting was initiated at a relatively negative potential and  $E_{prot}$  is only approximately 100mV more positive than  $E_{cor}$  (see Table 3-2).

Table 3-2  
Values for  $E_{cor}$ ,  $E_{pit}$ , and  $E_{prot}$  for Type 317L Stainless Steel Measured by CPP Experiments

Solution	Interface	Scan Rate, V/h	Pitting Sites	$E_{cor}$ V (SCE)	$E_{pit}$ V (SCE)	$E_{prot}$ V (SCE)
E1	H/S	0.6	I S	+0.15	+0.70(R)	+0.12
E1	H/S	0.06	I (S)	+0.20	+0.40	0.00
E1	V/L	0.6	S	+0.25	+0.51	NA
E1	V/L	0.6	S	+0.21	+0.58	+0.08
E1	V/L	0.06	S	+0.22	+0.44	0.00
E2	H/S	0.6	(I) S	-0.22	+0.06	-0.11
E2	H/S	0.06	(I) S	-0.15	-0.02	-0.08
E2	V/L	0.6	S	+0.02	+0.12	+0.01
E2	V/L	0.06	S	-0.20	-0.01	-0.08
E3	H/S	0.6	I S	+0.01	+0.68	-0.05
E3	H/S	0.6	I (S)	-0.12	+0.78	-0.05
E3	H/S	0.06	I (S)	+0.06	+0.82	-0.17
E3	H/S	0.06	I (S)	+0.02	+0.34	-0.08
E3	V/L	0.6	S	-0.14	+0.54	+0.02
E3	V/L	0.06	S	-0.16	+0.84	-0.02

R: Pitting initiated during reverse scan.

I: Pits initiated at PTFE holder/specimen interface.

S: Pits initiated on general surface away from any interface.

( ): Less favored pit initiation site.

NA: Data not available.

H/S: PTFE holder/specimen interface used in test.

V/L: Vapor/liquid interface used in test.

Figure 3-7 shows the CPP curve for 317L in Solution E2 with a PTFE holder/specimen interface and performed at a scan rate of 0.06V/h. Very little, if any, preferential pitting was associated with the PTFE holder/specimen interface. Comparison of the fast scan (0.6V/h) shown in Figure 3-6 to the slow scan (0.06V/h) shown in Figure 3-7 indicates a more negative  $E_{pit}$  was observed for the slow scan test. Also, a significant amount of current fluctuation was observed for the slow-scan test prior to initiation of stable pitting. The protection potential for the slow scan test was only 30mV more positive than for the fast scan test.

Figure 3-8 shows the CPP curve for 317L in Solution E2 with a vapor/liquid interface and performed at a scan rate of 0.6V/h. No preferential pitting was observed at the vapor/liquid interface. Comparing the CPP curve in

Figure 3-8 to that shown in Figure 3-6 indicates that  $E_{pit}$  and  $E_{prot}$  values for the specimen with a vapor/liquid interface are more positive than for the specimen with a PTFE holder/specimen interface.

Figure 3-9 shows the CPP curve for 317L in Solution E2 with a vapor/liquid interface and performed at a scan rate of 0.06V/h. No preferential pitting was observed at the vapor/liquid interface. Comparing the CPP curve in Figure 3-9 (vapor/liquid interface: 0.06V/h) with that in Figure 3-8 (vapor/liquid interface: 0.6V/h) indicates  $E_{pit}$  and  $E_{prot}$  are more negative for the slow scan rate (130mV and 90mV, respectively). Comparing the CPP curve in Figure 3-9 (vapor/liquid interface: 0.06V/h) to that shown in Figure 3-7 (PTFE holder/specimen interface: 0.06V/h) indicates almost identical behavior with  $E_{pit}$  and  $E_{prot}$  values within 20mV for the two curves.

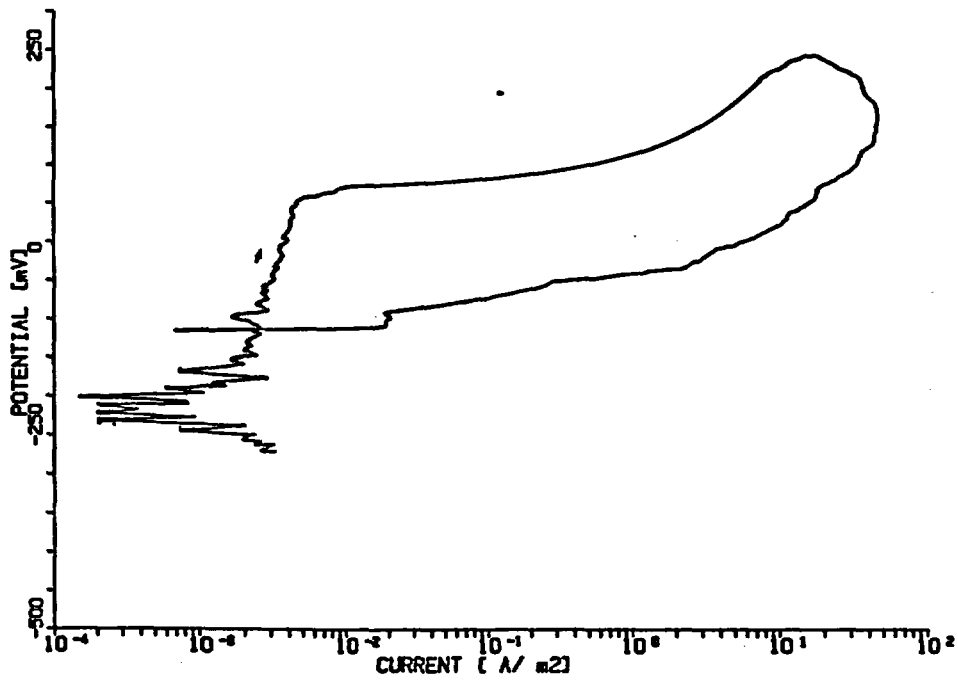


Figure 3-6. CPP Curve for Type 317L Stainless Steel in Solution E2 With a PTFE Holder/Specimen Interface Performed at a Scan Rate of 0.6V/h

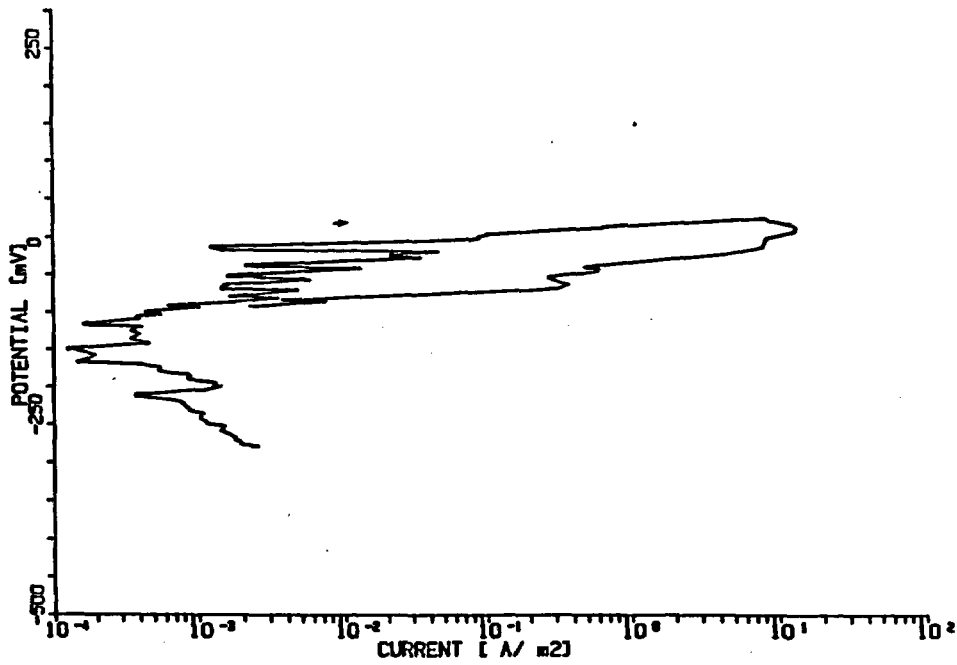


Figure 3-7. CPP Curve for Type 317L Stainless Steel in Solution E2 With a PTFE Holder/Specimen Interface Performed at a Scan Rate of 0.06V/h

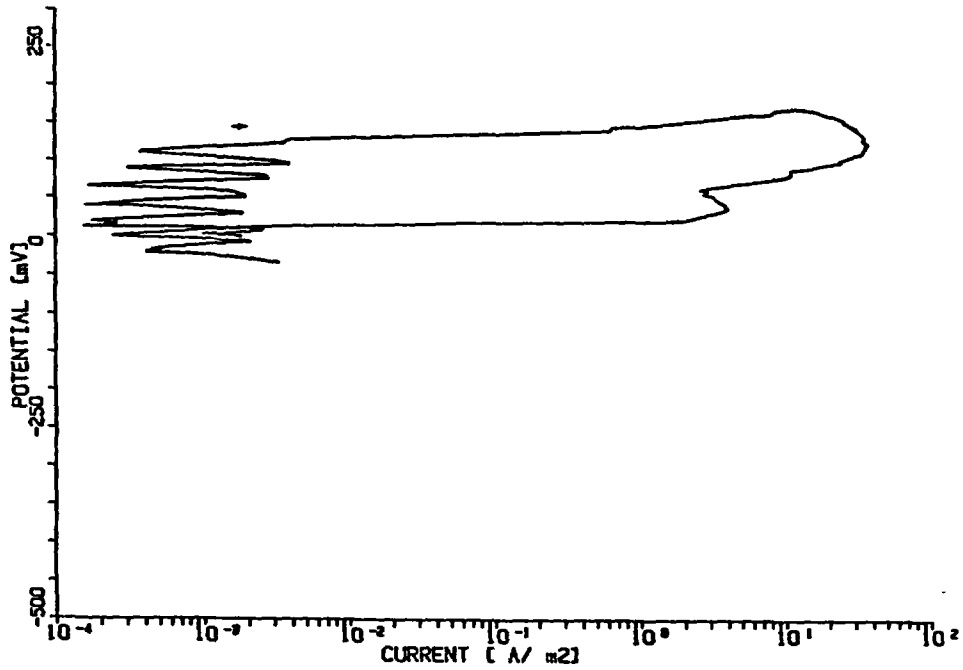


Figure 3-8. CPP Curves for Type 317L Stainless Steel in Solution E2 With a Vapor/Liquid Interface Performed at a Scan Rate of 0.6V/h

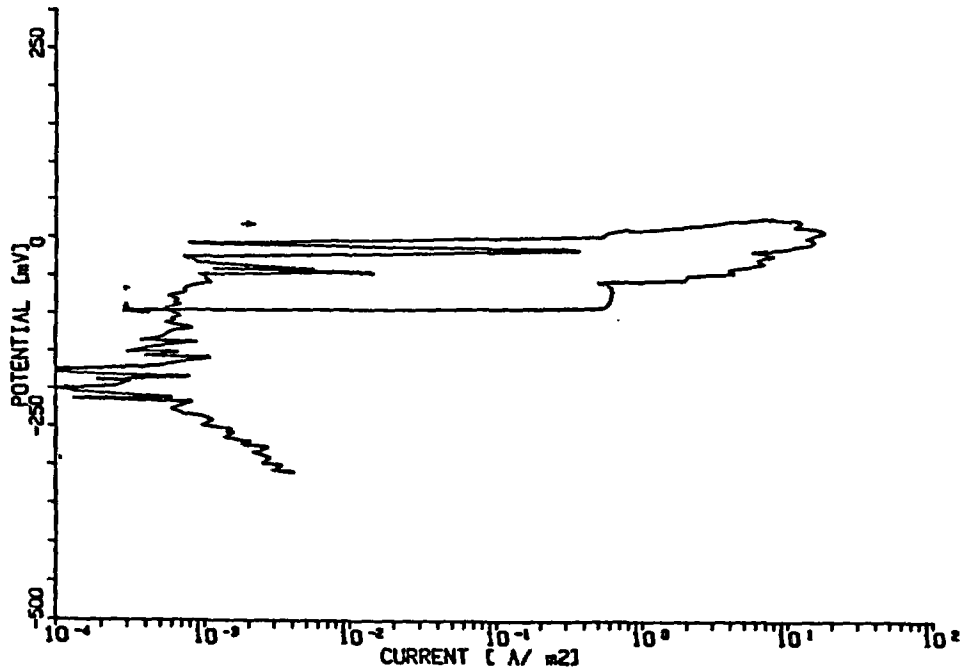


Figure 3-9. CPP Curves for Type 317L Stainless Steel in Solution E2 With a Vapor/Liquid Interface Performed at a Scan Rate of 0.06V/h

### Solution E3

Figure 3-10 shows CPP curves for duplicate specimens of 317L in Solution E3 with a PTFE holder/specimen interface and performed at a scan rate of 0.6V/h. Pitting was observed on specimens in both tests at the PTFE holder/specimen interface.  $E_{pit}$  values for the two curves are 100mV apart, while  $E_{prot}$  values are identical. As can be seen from the curves, a very large hysteresis is observed with  $E_{prot}$  similar to  $E_{cor}$

Figure 3-11 shows the CPP curves for duplicate specimens of 317L in Solution E3 with a PTFE holder/specimen interface and performed at a scan rate of 0.06V/h. Preferential pitting was observed at the PTFE holder/specimen interface for both specimens shown in Figure 3-11. A significant difference is observed in  $E_{pit}$  (480mV) for the two curves and a difference of 90mV is observed in  $E_{prot}$ . Comparison of the CPP curves shown in Figure 3-11 to those shown in Figure 3-10 indicate that the protection potentials are similar for the different scan rates. Because of the large variation in  $E_{pit}$  for the duplicate tests shown in Figure 3-11, it is difficult to draw conclusions as to the effect of scan rate on  $E_{pit}$ .

Figure 3-12 shows the CPP curve for 317L in Solution E3 with a vapor/liquid interface and performed at a scan rate of 0.6V/h. No preferential pitting was observed at the vapor/liquid interface. Comparing the CPP curve in Figure 3-12 (vapor/liquid interface: 0.6V/h) with that in Figure 3-10 (PTFE holder/specimen interface: 0.6V/h) indicates that  $E_{pit}$  for the vapor/liquid interface is slightly more negative than for the specimens with a PTFE holder/specimen interface, and  $E_{prot}$  for the vapor/liquid interface is 70mV more positive than for the specimens with a PTFE holder/specimen interface.

Figure 3-13 shows the CPP curve for 317L in Solution E3 with a vapor/liquid interface and performed at a scan rate of 0.06V/h. No preferential pitting was observed at the vapor/liquid interface. Comparison of the CPP curve in Figure 3-13 (vapor/liquid interface: 0.06V/h) with that in Figure 3-12 (vapor/liquid interface: 0.06V/h) indicates that  $E_{pit}$  is more negative for the faster scan rate. This finding is contradictory to the hypothesis that a slower scan rate should provide for longer incubation times and, thereby, generally have a more negative  $E_{pit}$ . The protection potential for the curves at the two scan rates are very similar (within 50mV).

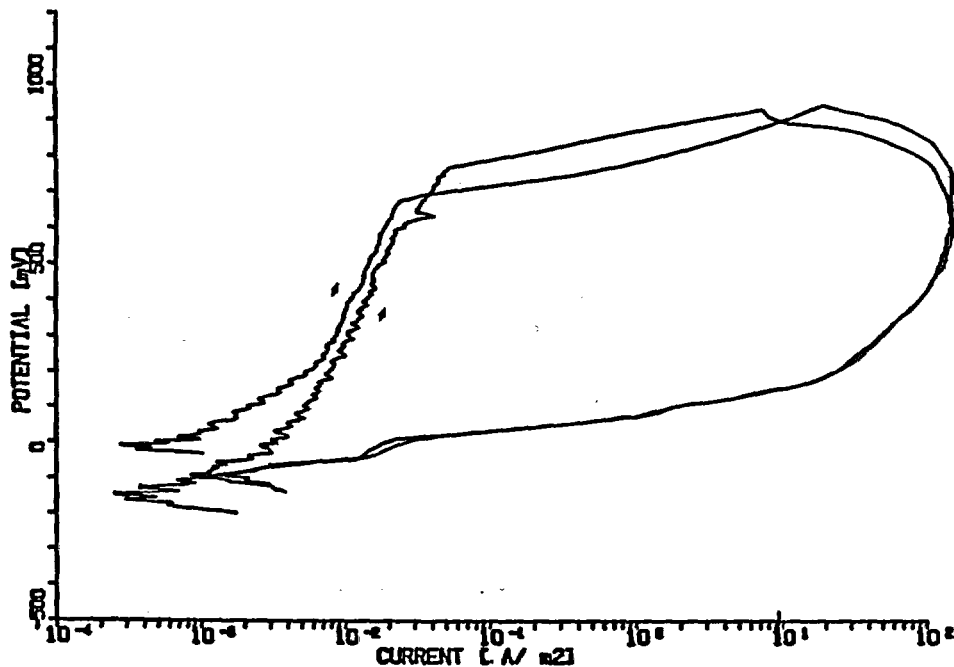


Figure 3-10. CPP Curve for Type 317L Stainless Steel in Solution E3 With a PTFE Holder/Specimen Interface Performed at a Scan Rate of 0.6V/h

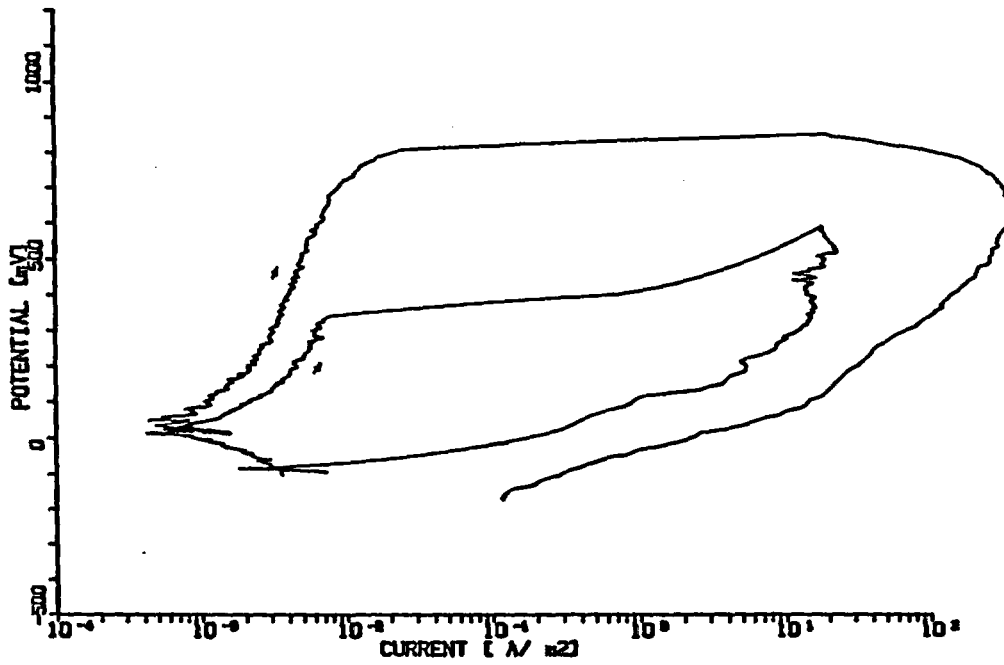


Figure 3-11. CPP Curve for Type 317L Stainless Steel in Solution E3 With a PTFE Holder/Specimen Interface Performed at a Scan Rate of 0.06V/h

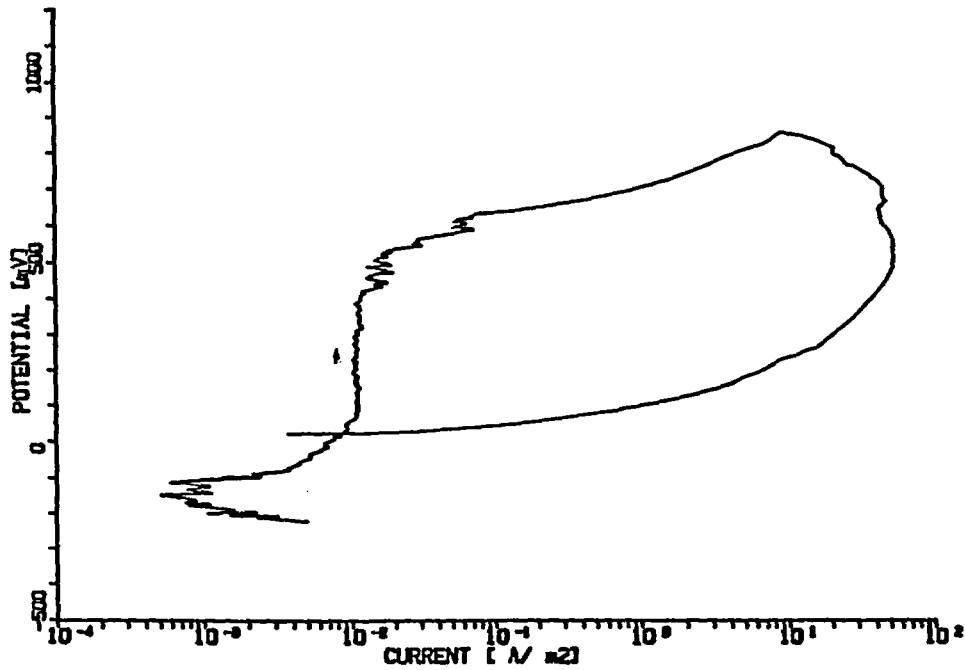


Figure 3-12. Curves for Type 317L Stainless Steel in Solution E3 With a Vapor/Liquid Interface Performed at a Scan Rate of 0.6V/h

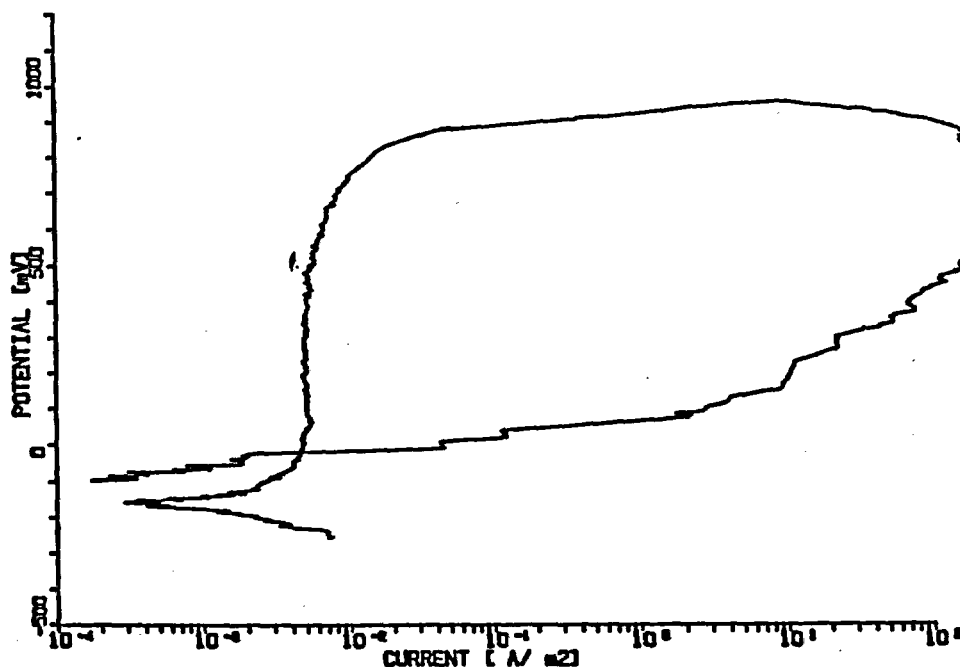


Figure 3-13. CPP Curves for Type 317L Stainless Steel In Solution E3 With a Vapor/Liquid Interface Performed at a Scan Rate of 0.06V/h

### Results for Alloy G3

Alloy G3 was tested in two solutions: E4 and E5. For each solution, CPP curves are presented for four conditions: specimen with PTFE holder/specimen interface at scan rates of 0.6V/h and 0.06V/h, and specimen with vapor/liquid interface at scan rates of 0.6V/h and 0.06V/h.

#### Solution E4

Figure 3-14 shows a CPP curve for Alloy G3 in Solution E4 with a PTFE holder/specimen interface and performed at a scan rate of 0.6V/h. Preferential pitting was observed at the PTFE holder/specimen interface for one of the specimens. Table 3-3 presents  $E_{cor}$ ,  $E_{pit}$ ,  $E_{prot}$ , and location of pitting for Alloy G3 specimens in Solutions E4 and E5.

Figure 3-15 shows the CPP curve for Alloy G3 in Solution E4 with a PTFE holder/specimen interface and performed at a scan rate of 0.06V/h. No preferential pitting was observed at the PTFE holder/specimen interface. Comparing the CPP curve in Figure 3-15 with that shown in Figure 3-14 indicates  $E_{prot}$  is somewhat more negative for the slow scan than the fast scan. The value

of  $E_{pit}$  is much more negative for the slow scan test, which is the expected result.

Figure 3-16 shows the CPP curve for Alloy G3 in Solution E4 with a vapor/liquid interface and performed at a scan rate of 0.6V/h. The very small hysteresis loop observed is not associated with pitting and no pits were observed on the specimen surface. This is in stark contrast to the 0.6V/h scan rate tests performed with a PTFE holder/specimen interface in which pitting was observed. However, the pitting in the PTFE holder/specimen tests was associated with the PTFE holder/specimen interface. Therefore, for the Alloy G3 in Solution E4, it appears that the PTFE holder/specimen interface greatly enhances the initiation of pitting.

Figure 3-17 shows the CPP curves for duplicate specimens of G3 in Solution E4 with a vapor/liquid interface and performed at a scan rate of 0.06V/h. In one of the curves (broken line), no pitting was observed with only a small hysteresis loop at the very positive potentials, while for the other curve (solid line), pitting initiated on the reverse scan at about 0.6V (SCE). Severe pitting over the entire surface area was observed with no preferential attack at the vapor/liquid interface. This was only the



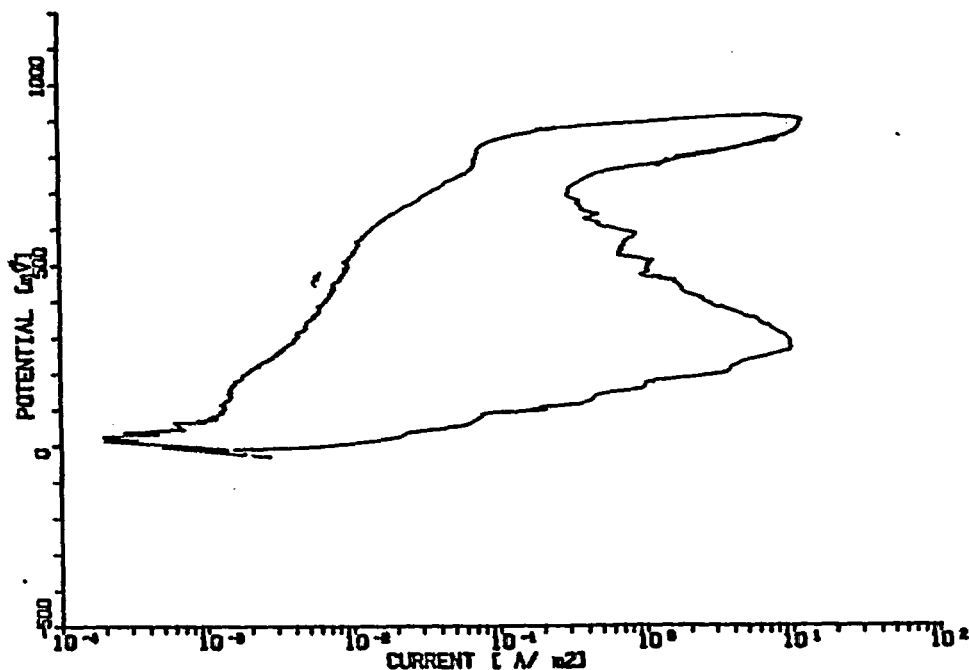


Figure 3-14. CPP Curves for Alloy G3 in Solution E4 With a PTFE Holder/Specimen Interface Performed at a Scan Rate of 0.6V/h

Table 3-3  
Values for  $E_{cor}$ ,  $E_{pit}$ , and  $E_{prot}$  for Alloy G3 Measured by CPP Experiments

Solution	Interface	Scan Rate, V/h	Pitting Sites	$E_{cor}$ V (SCE)	$E_{pit}$ V (SCE)	$E_{prot}$ V (SCE)
E4	H/S	0.6	I	+0.02	+0.70(R)	0.00
E4	H/S	0.06	S	-0.18	+0.20	-0.14
E4	V/L	0.6	None	-0.16	NP	NP
E4	V/L	0.06	None	-0.02	NP	NP
E4	V/L	0.06	S	-0.19	+0.59(R)	+0.13
E5	H/S	0.6	I	+0.16	+0.35	-0.05
E5	H/S	0.6	I	-0.15	+0.28	-0.05
E5	H/S	0.06	I	+0.25	+0.80	+0.01
E5	V/L	0.6	None	+0.14	NP	NP
E5	V/L	0.06	None	+0.10	NP	NP

R: Pitting initiated during reverse scan.  
 I: Pits initiated at PTFE holder/specimen interface.  
 S: Pits initiated on general surface away from any interface.  
 ( ): Less favored pit initiation site.  
 NP: No pitting, hence no  $E_{pit}$  or  $E_{prot}$ .  
 H/S: PTFE holder/specimen interface used in test.  
 V/L: Vapor/liquid interface used in test.

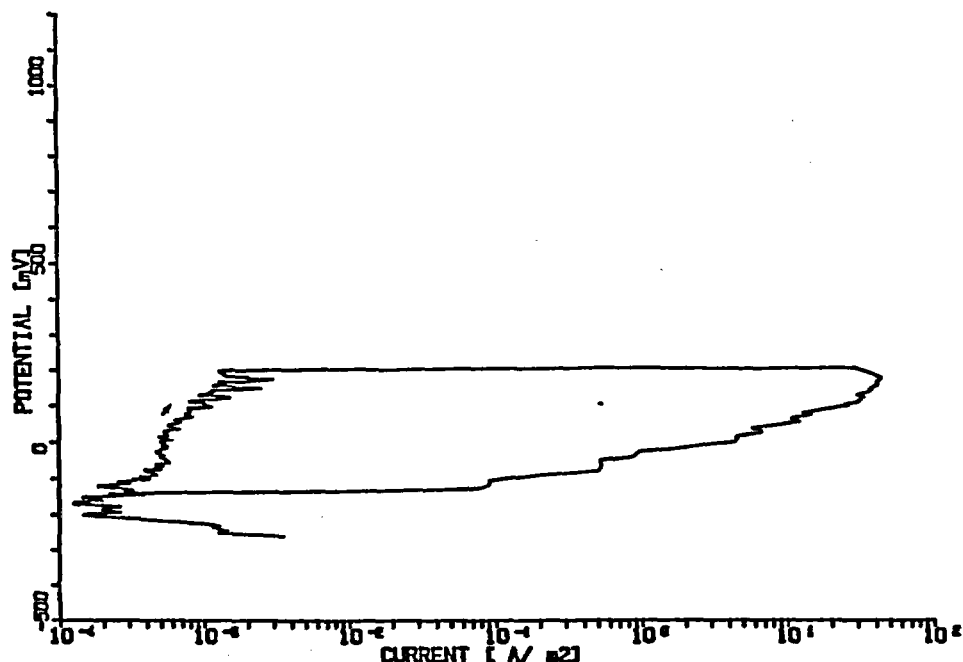


Figure 3-15. CPP Curves for Alloy G3 In Solution E4 With a PTFE Holder/Specimen Interface Performed at a Scan Rate of 0.06V/h

second specimen out of the six CPP experiments with Alloy G3 that exhibited pitting on the free surface. The specimens for all of these tests were cut from the same piece of material and the pH of the solutions was checked to establish that an error in the solution makeup had not occurred. It is not known whether surface contamination or some other experimental procedure caused the pitting on the free surface for these two specimens. The specimens were all prepared in the same manner, which included the use of new polishing/grinding paper. Therefore, it was highly unlikely that surface contamination occurred during the grinding of the specimen down to a 600-grit surface. It is obvious that the presence or lack of a preferred pit-initiation site (PTFE holder/specimen interface) is very important to the results of the CPP experiments for the nickel alloy in Solution E4. Furthermore, the incubation time for pitting may be exceedingly long in the absence of a preferred pit-initiation site.

#### Solution E5

Figure 3-18 shows the CPP curves for duplicate specimens of Alloy G3 in Solution E5 with a PTFE holder/specimen interface and performed at a scan rate of 0.6V/h. Preferential pitting was observed at the PTFE holder/

specimen interface. The initial breakdown for the two tests indicate a value of  $E_{pit}$ , which is less than 100mV apart. The values for  $E_{prot}$  for the two tests are identical.

Figure 3-19 shows the CPP curve for Alloy G3 in Solution E5 with a PTFE holder/specimen interface and performed at a scan rate of 0.06V/h. Preferential pitting was observed at the PTFE holder/specimen interface. Comparing the CPP curve in Figure 3-19 with that in Figure 3-18 indicates that pit initiation occurred at a more positive value for the slow scan test than for the fast scan test. This is not typical and is likely due to preferential pitting sites being different for the specimens. The values for  $E_{prot}$  for the two scan rates are within 60mV.

Figure 3-20 shows the CPP curve for Alloy G3 in Solution E5 with a vapor/liquid interface and performed at a scan rate of 0.6V/h. As was observed for Alloy G3 in Solution E4, once the PTFE holder/specimen interface was removed, pits did not initiate on the Alloy G3 surface.

Figure 3-21 shows the CPP curve for Alloy G3 in Solution E5 with a vapor/liquid interface and performed at a scan rate of 0.06V/h. Once again, it was observed that no pitting occurred for Alloy G3 in Solution E5 when the PTFE holder/specimen interface was not present.

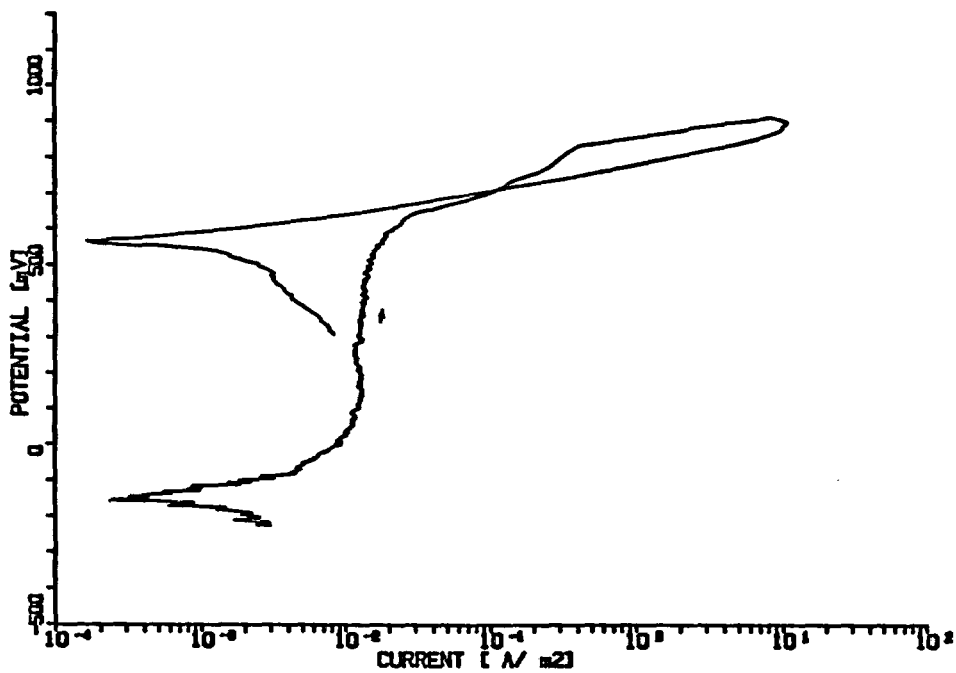


Figure 3-16. CPP Curves for Alloy G3 In Solution E4 With a Vapor/Liquid Interface Performed at a Scan Rate of 0.6V/h

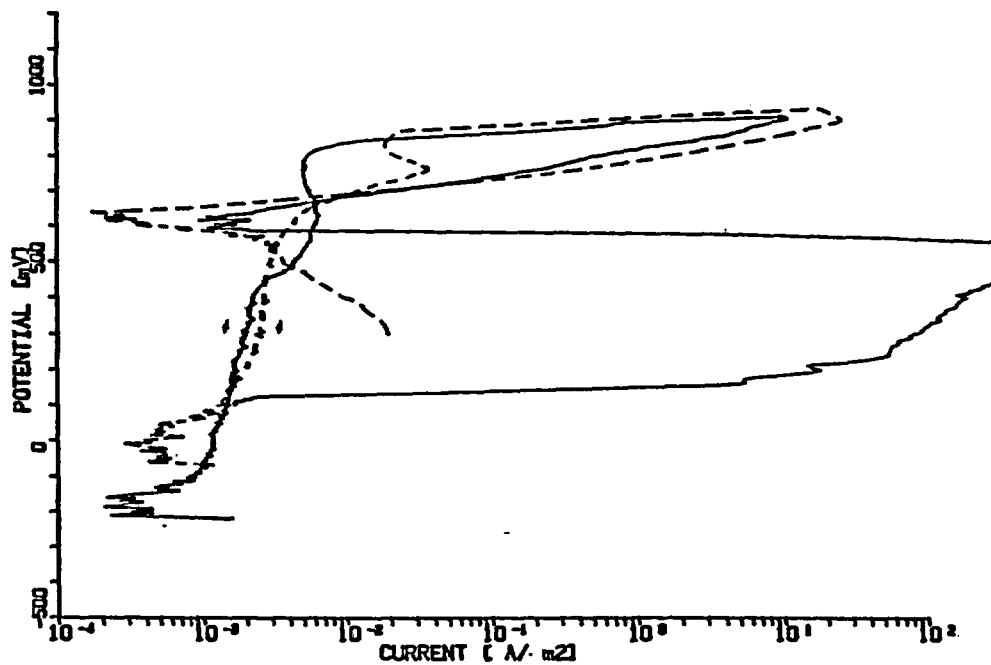


Figure 3-17. CPP Curves for Alloy G3 In Solution E4 With a Vapor/Liquid Interface Performed at a Scan Rate of 0.06V/h

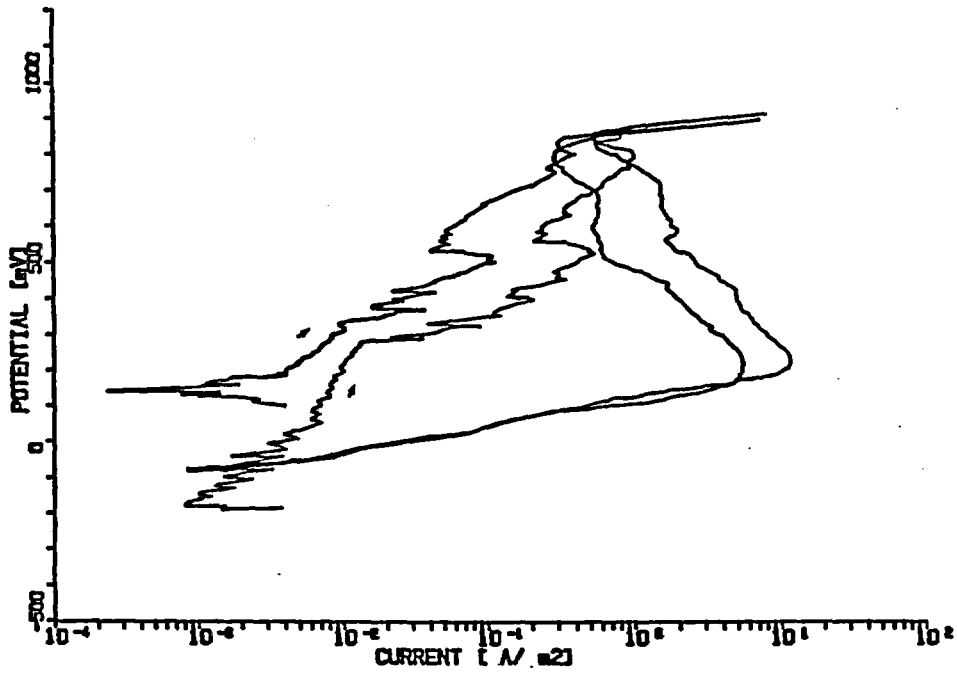


Figure 3-18. CPP Curves for Alloy G3 In Solution E5 With A PTFE Holder/Specimen Interface Performed at a Scan Rate of 0.6V/h

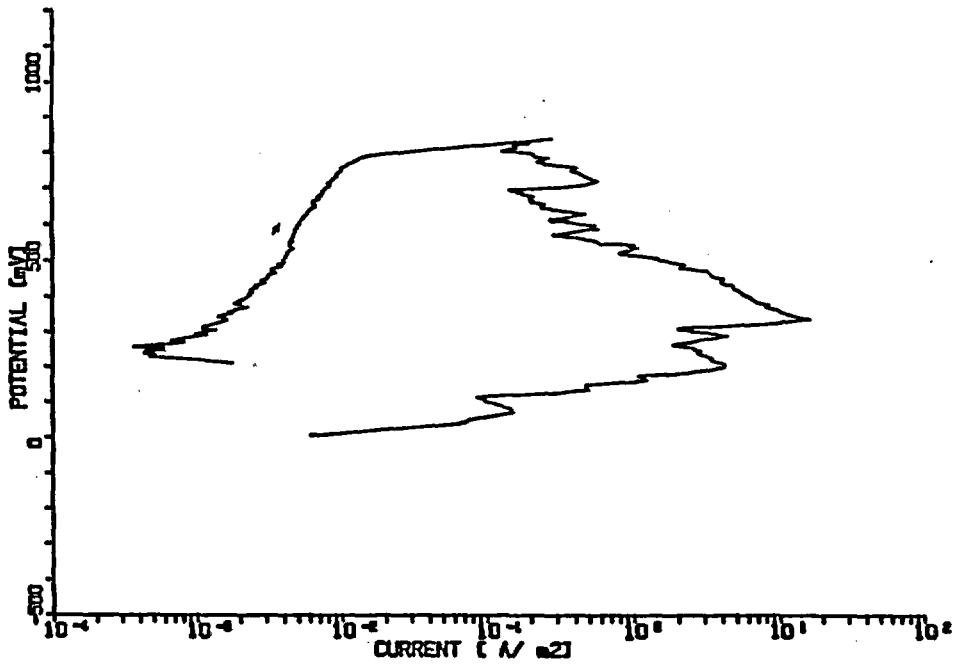


Figure 3-19. CPP Curves for Alloy G3 In Solution E5 With a PTFE Holder/Specimen Interface Performed at a Scan Rate of 0.06V/h

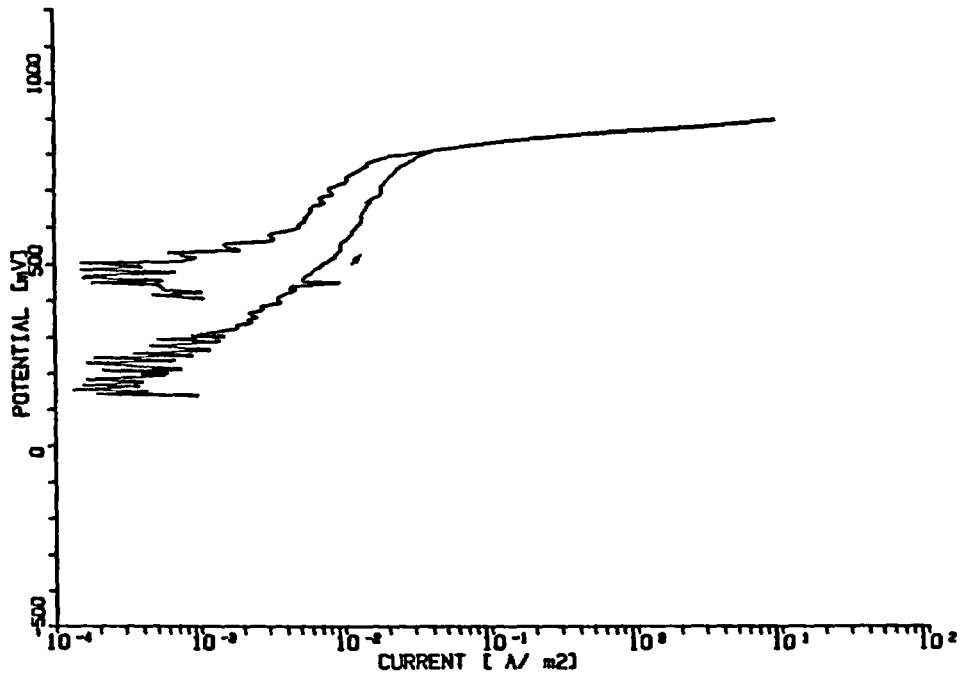


Figure 3-20. CPP Curves for Alloy G3 In Solution E5 With a Vapor/Liquid Interface Performed at a Scan Rate of 0.6V/h

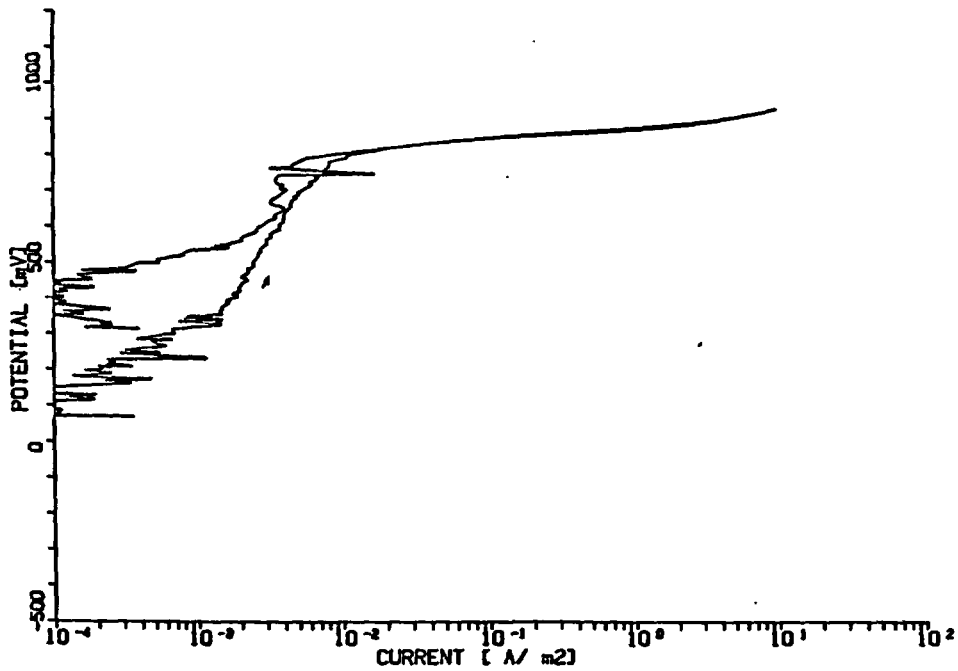


Figure 3-21. CPP Curves for Alloy G3 In Solution E5 With a Vapor/Liquid Interface Performed at a Scan Rate of 0.06V/h

# 4

## CONSTANT POTENTIAL-TIME EXPERIMENTS

---

The purpose of these experiments was to establish the potential at which stable pit initiation occurs while maintaining the specimen at a constant potential in the range between  $E_{pit}$  and  $E_{prot}$ . Two alloy-solution combinations were selected for examination in this task: Type 317L stainless steel in Solution E3 and Alloy G3 in Solution E4.

### Experimental Approach

The experimental procedures were relatively simple. The specimen configuration was similar to that described in Section 3, i.e., cylindrical specimen mounted on a PTFE holder with either a PTFE holder specimen interface immersed in the solution or the presence of a vapor/liquid interface on the specimen surface. Specimens were immersed in the solution and permitted to stabilize for approximately 20 hours before polarizing to the desired potential. Polarization was accomplished with either Thompson Electrochem Microstats or Cortest Instrument Systems Model 2125 potentiostats. Two compartment PTFE electrochemical cells having a combined working-counter compartment and a separate reference electrode compartment were used.

Current measurements were made as the voltage drop across a resistor placed in series in the counter electrode lead. The resistor was varied from  $10^2$  to  $10^6$  ohms, depending on the magnitude of the current. The voltage

drop across the resistor was recorded on a strip chart recorder for the initial 24 to 48 hours and switched to a computer data acquisition for sampling every 15 minutes. The primary data desired were the times to stable pit initiation. Typical currents, prior to pit initiation, for passive conditions were  $10^{-5}$  to  $10^{-4}$  A/m<sup>2</sup>. Upon pit initiation, the current increased to as high as 2.4 A/m<sup>2</sup>. Therefore, it was typically quite easy to establish the time-to-pit initiation by monitoring current.

### Results for Type 317L Stainless Steel in Solution E3

Table 4-1 presents the time-to-pit initiation data for the constant potential-time tests. The tests for the vapor/liquid interface will be considered first. No pitting occurred preferentially at the interface in any of these tests. At a potential of 0.4V (SCE) pits initiated between 23 and 619 hours following application of the potential. With the exception of Test No. 3106, at 0.3V (SCE), no pit initiation had occurred after up to 1658 hours. Test No. 3106 is considered as a separate case because it was much more active (negative free-corrosion potential) when the test was initiated than any of the other tests. The more active behavior prior to application of the constant potential was attributed to a much longer (16 hours) purging of N<sub>2</sub> than normal (1 hour) prior to immersing the test specimen. This emphasizes the sensitivity of the pit initiation process to changes in test conditions.

**Table 4-1**  
**Data for Constant Potential-Time Experiments for Type 317L Stainless Steel in Solution E3**

Test No.	Interface Present <sup>(a)</sup>	Polarized Potential, V, (SCE)	Time-to-Pit Initiation, Minutes
3097	V/L	+0.20	$>4.0 \times 10^4$ <sup>(b)</sup>
0103A	H/S	+0.20	$>9.0 \times 10^4$ <sup>(b)</sup>
3123	H/S	+0.30	$2.0 \times 10^3$
0103B	H/S	+0.30	$9.4 \times 10^2$
3126	H/S	+0.30	$>1.1 \times 10^5$ <sup>(b)</sup>
3102	V/L	+0.30	$>7.3 \times 10^3$ <sup>(b)</sup>
3104	V/L	+0.30	$>1.0 \times 10^5$ <sup>(b)</sup>
3105	V/L	+0.30	$>9.1 \times 10^4$ <sup>(b)</sup>
3106	V/L	+0.30	$4.1 \times 10^3$ <sup>(c)</sup>
NA	V/L	+0.40	$1.2 \times 10^4$
3099	V/L	+0.40	$3.7 \times 10^4$
3100	V/L	+0.40	$1.4 \times 10^3$

(a) V/L: Vapor/liquid interface.

H/S: PTFE holder/specimen interface.

(b) Test terminated after number of minutes shown, no pitting.

(c) Specimen had an unusually active free-corrosion potential prior to application of constant potential (see text).

NA: Data collected prior to setting up computerized data acquisition system.

Three tests were performed with PTFE holder/specimen interfaces immersed in the test solution at 0.3V (SCE). Two of these tests initiated pitting following only 34 hours and 16 hours, while the other specimen exhibited no pitting after 1876 hours. These data indicate the wide scatter to be expected in pit initiation tests. Based on the above results, pits initiate at potentials more noble than 0.2 to 0.3V (SCE). Furthermore, the presence of the PTFE holder/specimen interface provides a preferred pit initiation site that increases the possibility of pitting.

Recalling data from the CPP tests (Table 3-2),  $E_{pit}$  and  $E_{prot}$  were in the range of 0.75 to 0.34V (SCE) and -0.05 to -0.17V (SCE) respectively, when a PTFE holder/specimen interface was present. The most negative value for  $E_{pit}$  (0.34V) was recorded on one of the slow scan (0.06V/h) curves. When a vapor/liquid interface was present,  $E_{pit}$  and  $E_{prot}$  were in the range of 0.84 to 0.54V (SCE) and 0.02 to -0.02V (SCE), respectively. Therefore, the value of  $E_{pit}$  from the constant potential-time tests is slightly more negative than the most negative value determined by the CPP tests. Also,  $E_{pit}$  determined by the

constant potential-time tests was still significantly more positive than the value of  $E_{prot}$  determined by the CPP tests.

### Results for Alloy G3 in Solution E4

Table 4-2 presents the time-to-pit initiation data for the constant-potential tests for Alloy G3 in Solution E4. The specimens with the vapor/liquid interface will be considered first. With only a vapor/liquid interface present, pits were not initiated for specimens at 0.6 or 0.4V (SCE) after 1500 hours. At a potential of 0.8V (SCE), pits initiated after 138 hours. However, if a crevice collar (similar to the one used in ASTM standard test method F-746) was placed on the specimens, crevice corrosion was observed at 0.6V after exposure periods of 73 and 1081 hours. Therefore, the presence of the crevice provided preferred initiation sites for localized corrosion. It should be noted that the form of attack with the crevice collar was significantly different from that observed at the PTFE holder/specimen interface. Crevice corrosion occurred beneath the crevice collar, while pits were initiated at the PTFE holder/specimen interface.

**Table 4-2**  
**Data for Constant Potential-Time Experiments for Alloy G3 In Solution E4**

Test No.	Interface Present <sup>(a)</sup>	Polarized Potential, V, (SCE)	Time-to-Pit Initiation, Minutes <sup>(b)</sup>
3132	H/S	+0.20	$>1.0 \times 10^5$ <sup>(b)</sup>
3134	H/S	+0.20	$>8.9 \times 10^4$ <sup>(b)</sup>
3131	H/S	+0.30	$3.6 \times 10^0$
3125	H/S	+0.40	$4.8 \times 10^1$
3112	V/L	+0.40	$>9.5 \times 10^4$ <sup>(b)</sup>
3128	H/S	+0.50	$4.8 \times 10^1$
3124	H/S	+0.60	$2.4 \times 10^2$
3127	H/S	+0.60	$4.2 \times 10^1$
3113	V/L	+0.60	$>8.6 \times 10^4$ <sup>(b)</sup>
3133	V/L	+0.60	$>9.1 \times 10^4$ <sup>(b)</sup>
3115	Crevice, V/L	+0.60	$4.4 \times 10^3$
3116	Crevice, V/L	+0.60	$6.5 \times 10^4$
3114	V-L	+0.80	$8.3 \times 10^3$

(a) V/L: vapor/liquid interface  
 H/S: PTFE holder/specimen interface  
 Crevice: ASTM F746 crevice collar

(b) Test terminated after number of minutes shown, no pitting.

Several tests were performed with the PTFE holder/specimen interface present, which quite often provided a preferred site for pit initiation. At a potential of 0.6V (SCE), pits initiated after 4 and 0.7 hours. At potentials of 0.5, 0.4 and 0.3V (SCE) pits initiated in 0.8 hours or less. Two tests performed at 0.2V (SCE) indicated no pitting after 1684 and 1490 hours. With the PTFE holder/specimen interface present,  $E_{pit}$  from the constant potential tests was between 0.2V and 0.3V (SCE).

Recalling data from the CPP tests (Table 3-3),  $E_{pit}$  and  $E_{prot}$  were 0.70 to 0.20V (SCE) and 0.00 to -0.14V (SCE), respectively, when a PTFE holder/specimen interface

was present. When a vapor/liquid interface was present, no pitting at all was observed during two of the CPP tests, while one test exhibited values of  $E_{pit}$  and  $E_{prot}$  of 0.59 and 0.13V (SCE), respectively. The constant potential tests correspond reasonably well with the CPP tests, i.e., the presence of a preferred pit initiation site (PTFE holder/specimen interface) greatly increased the likelihood for pit initiation. Values of  $E_{pit}$  determined by constant potential-time tests were approximately equal to the most negative value of  $E_{pit}$  recorded by CPP tests. Also,  $E_{pit}$  determined by the constant potential-time tests was 0.3V more positive than the values of  $E_{prot}$  recorded for the CPP tests.



# 5

## MODIFIED ASTM F-746 TESTS

---

The purpose of these experiments was to examine the dependency of prior pitting history on the measured value of  $E_{\text{prot}}$ . The same two alloy-solution combinations were selected for examination in this task as were used in the constant potential-time experiments.

### Experimental Approach

Modified ASTM Standard F-746 tests were performed to determine  $E_{\text{prot}}$  while providing a well-controlled pitting history prior to determining  $E_{\text{prot}}$ . In this test, a critical variable is how much the largest active pit grows before it is repassivated. This largest pit is likely to control the potential,  $E_{\text{prot}}$ , of which repassivation occurs for that specimen. After considering several options and performing preliminary tests, it was decided that the total time at the pit stimulation potential (see below) was as good a measure of pit growth as total charge passed or time from rapid current increase.

Tests were performed utilizing a working electrode with the previously described PTFE holder/specimen interface. The test procedure was as follows: (1) insert test specimen; (2) permit to stabilize under freely corroding conditions (16–20 hours); (3) polarize to a potential of 0.60V to produce rapid onset of pitting; and (4) after a predetermined time for pitting, polarize the specimen to a more negative potential and measure the current-time transient for up to 16 hours for the purpose of establishing  $E_{\text{prot}}$ . The above procedure was repeated until a potential was established above which pitting continued and below which complete repassivation occurred. As can be seen from the above procedures, modifications to the ASTM Standard F-746 are in three areas: (1) a crevice washer was not utilized, (2) the current criterion for

establishing the pitting history was replaced by a specified time, and (3) the length of time for monitoring the current transient at  $E_{\text{prot}}$  was extended from 15 minutes to several hours.

### Results for Type 317L Stainless Steel In Solution E3

The time of pitting was the primary variable in the test matrix. Following a specified time of pitting, the potential was stepped to a potential close to the value of  $E_{\text{prot}}$  determined in CPP tests. By performing several such tests at different potentials, an independent value of  $E_{\text{prot}}$  was established as the most noble (positive) potential at which pits, initiated at +0.60V, repassivated. Upon polarization to +0.60V, a large current transient occurred, followed by a decrease in current to a minimum, followed by a current increase indicating significant pitting. Preliminary experiments showed that pits initiate even during the initial current transient and subsequent current decrease. Therefore, pitting time was calculated from the initial polarization to +0.60V (SCE).

Figures 5-1 through 5-7 show current-time data following pit stimulation at +0.60V for selected periods and subsequent polarization at selected more negative potentials near the expected  $E_{\text{prot}}$  for alloy 317L.  $E_{\text{prot}}$  is defined as the potential below which repassivation occurs and above which pits grow. For instance, in Figure 5-1,  $E_{\text{prot}}$  was determined to be in the range of 150 to 200mV (SCE). Table 5-1 summarizes the data as a function of pitting time. It is seen that  $E_{\text{prot}}$  became more positive as pitting time decreased and leveled off at pitting times of less than 1 minute.

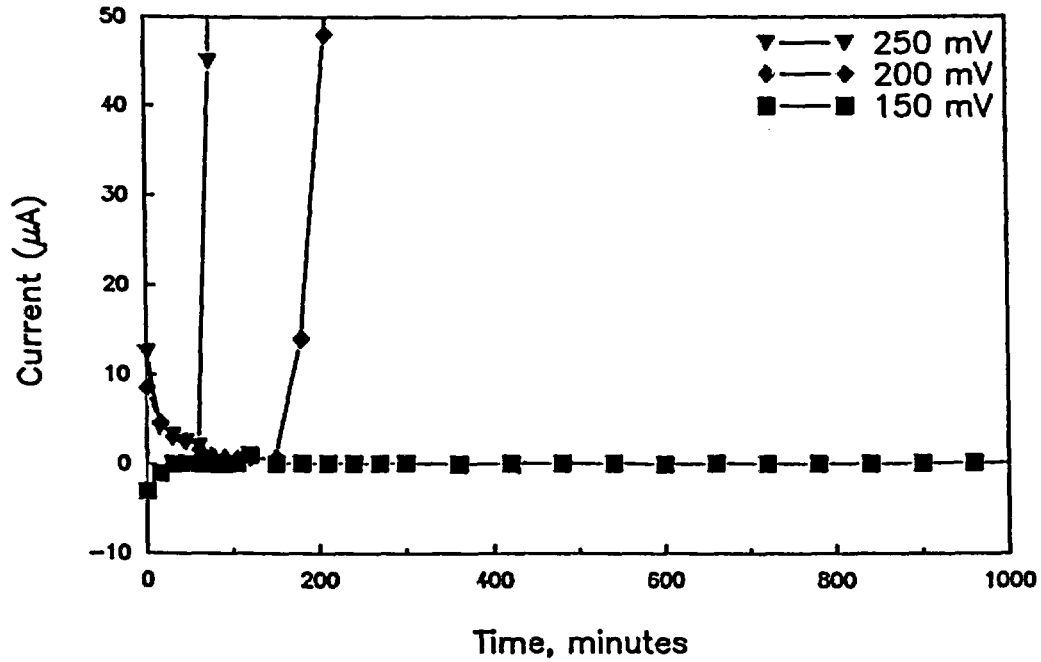


Figure 5-1. Current-Time Transients for Type 317L in Solution E3 Following Pit Stimulation at 0.6V (SCE) for 2 Seconds (0.03 min) and Polarized to a Potential Near  $E_{prot}$

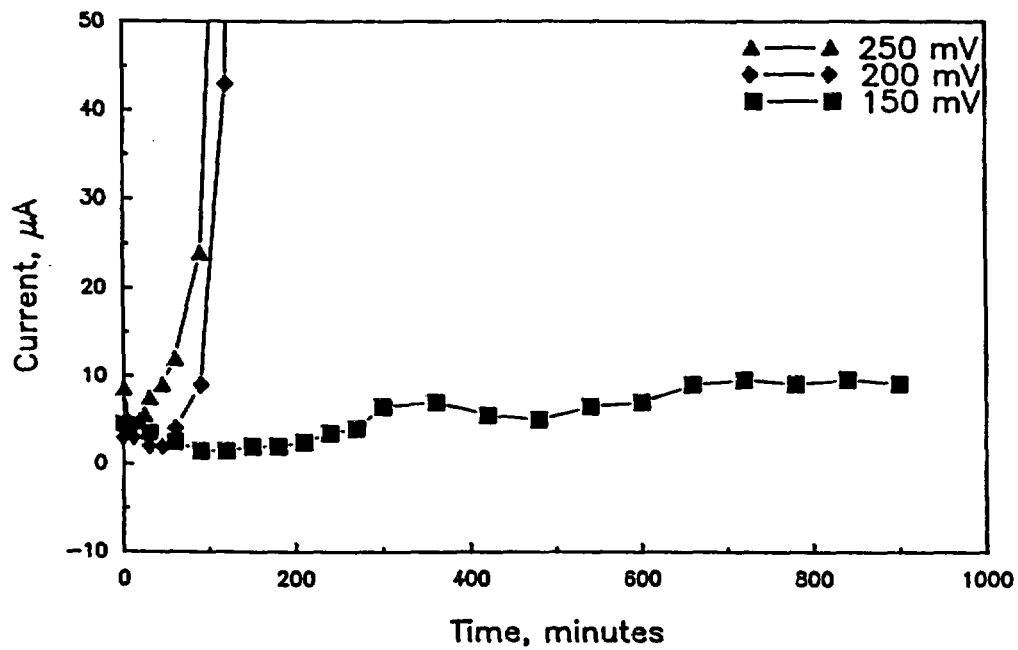


Figure 5-2. Current-Time Transients for Type 317L in Solution E3 Following Pit Stimulation at 0.6V (SCE) for 15 Seconds (0.25 min) and Polarized to a Potential Near  $E_{prot}$

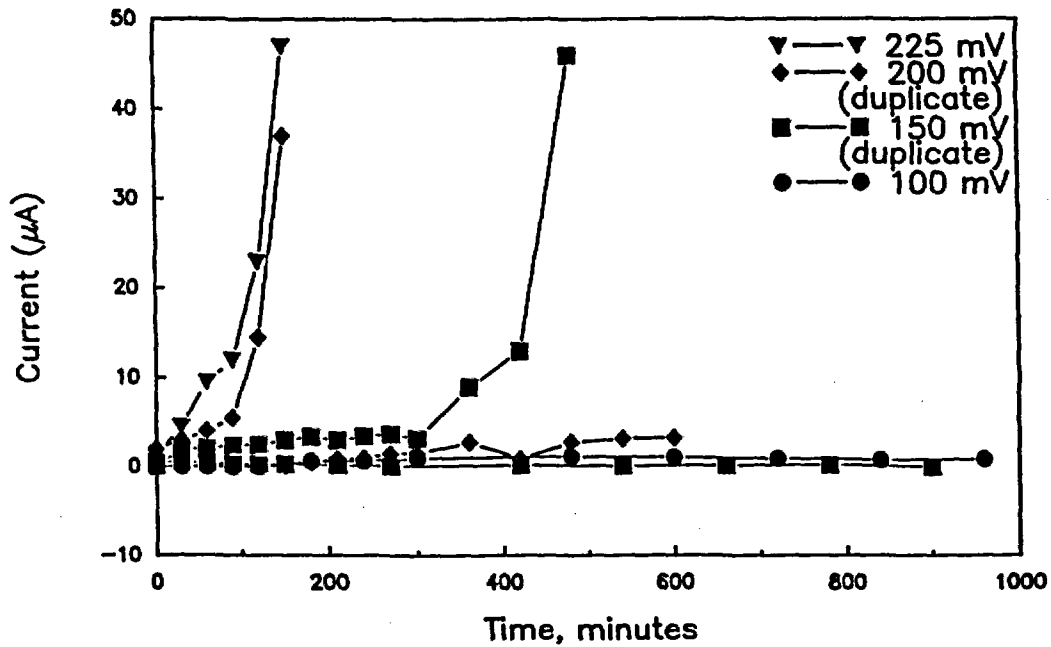


Figure 5-3. Current-Time Transients for Type 317L In Solution E3 Following Pit Stimulation at 0.6V (SCE) for 2 Minutes and Polarized to a Potential Near  $E_{prot}$  (Two Curves Shown for Duplicate Tests at 200mV and 150 mV)

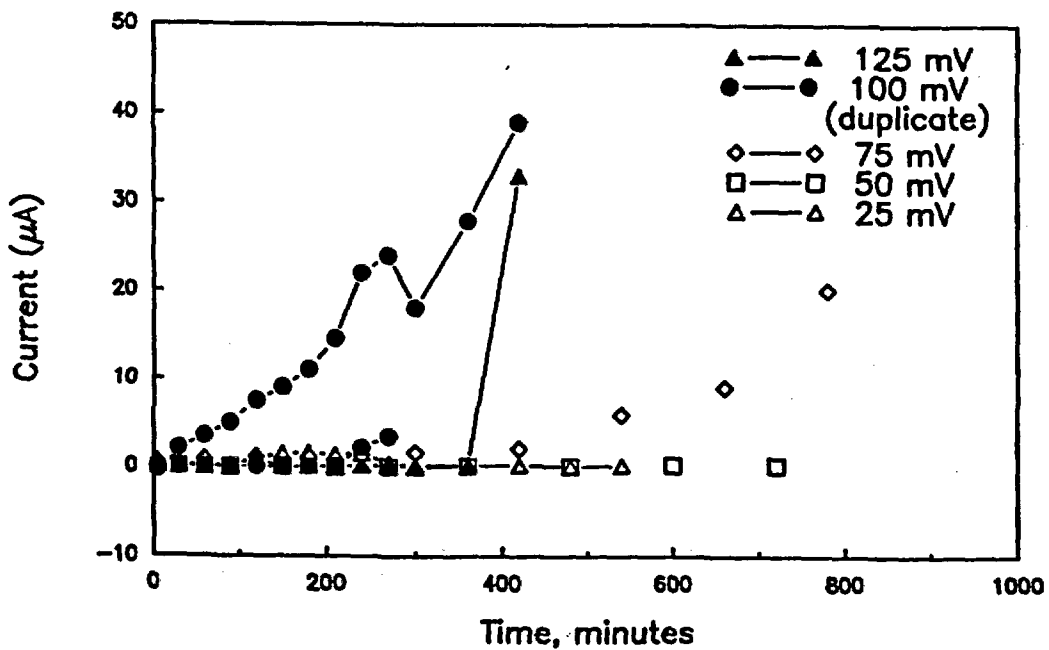


Figure 5-4. Current-Time Transients for Type 317L In Solution E3 Following Pit Stimulation at 0.6V (SCE) for 7 Minutes and Polarized to a Potential Near  $E_{prot}$  (Two Curves Shown for Duplicate Tests at 100 mV)

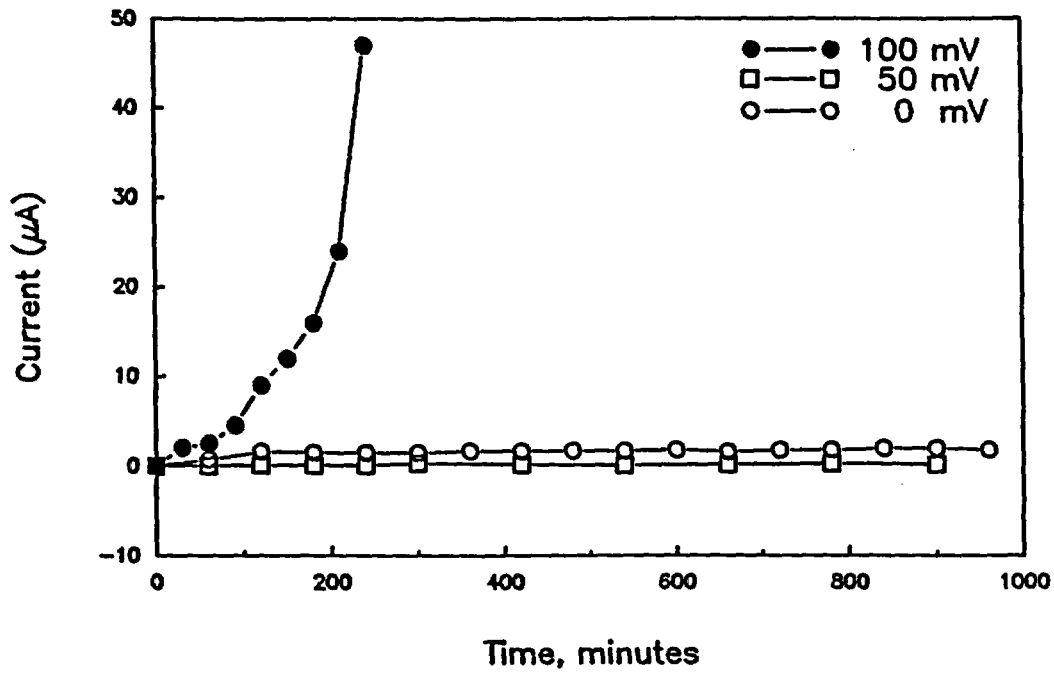


Figure 5-5. Current-Time Transients for Type 317L in Solution E3 Following Pit Stimulation at 0.6V (SCE) for 25 Minutes and Polarized to a Potential Near  $E_{prot}$

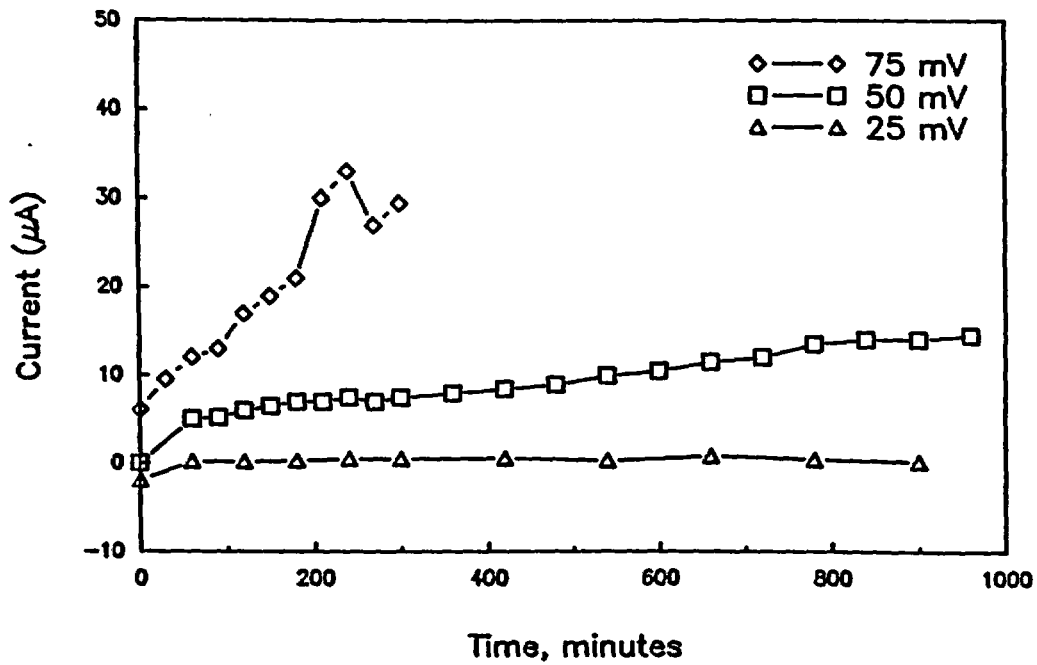


Figure 5-6. Current-Time Transients for Type 317L in Solution E3 Following Pit Stimulation at 0.6V (SCE) for 40 Minutes and Polarized to a Potential Near  $E_{prot}$

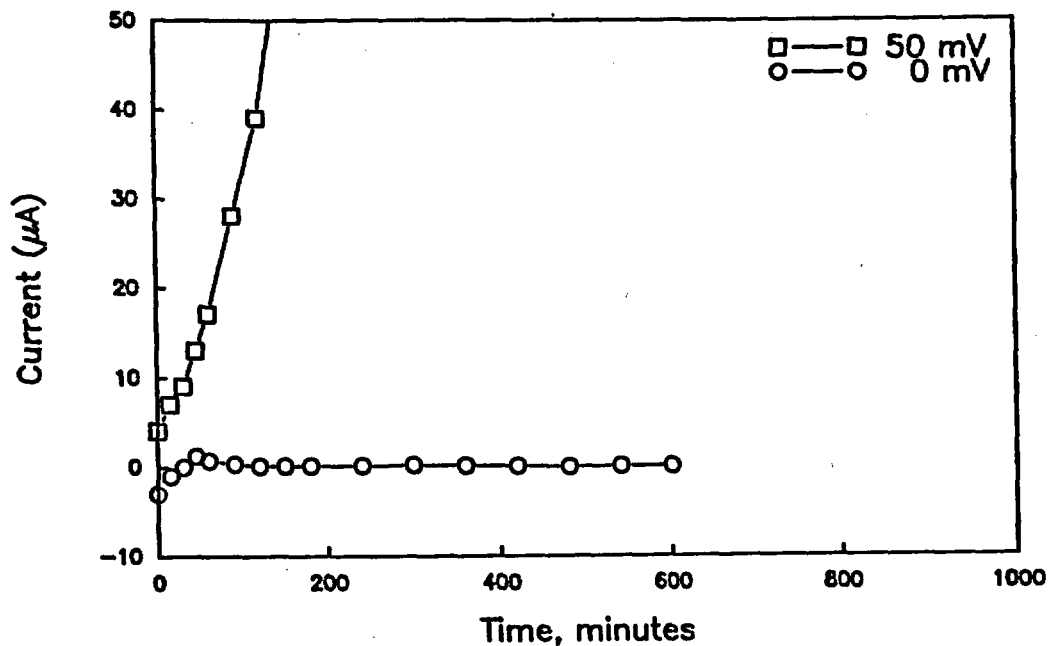


Figure 5-7. Current-Time Transients for Type 317L in Solution E3 Following Pit Stimulation at 0.6V (SCE) for 100 Minutes and Polarized to a Potential Near  $E_{\text{prot}}$

Table 5-1  
Values of  $E_{\text{prot}}$  as a Function of Time of Pitting From  
the Modified ASTM F-746 Tests

Alloy	Pitting Time, min.	$E_{\text{prot}}$ , mV, SCE
317L	0.03	+150 to +200
317L	0.25	+150 to +200
317L	2.0	+100 to +200
317L	7.0	+50 to +100
317L	25	+50 to +100
317L	40	+25 to +75
317L	100	0 to +50
G3	0.25	+50 to +100
G3	2.0	+50 to +100
G3	40	-50 to 0

#### Results for Alloy G3 in Solution E4

During polarization at +0.60V, the current-time behavior was very similar to that observed for Alloy 317L. Figures 5-8 through 5-10 show current-time data following pit stimulation at +0.60V (SCE) for selected periods and subsequent polarization at selected more negative potentials near the expected  $E_{\text{prot}}$  for Alloy G3.  $E_{\text{prot}}$  is determined for each "time of pitting" as the potential below which repassivation occurred and above which pits grow. Table 5-1 gives  $E_{\text{prot}}$  values as a function of pitting times at 0.06V (SCE). As for Alloy 317L, the value of  $E_{\text{prot}}$  became more positive with a decrease in pitting time from 40 to 2 minutes, but showed no further change for times less than 2 minutes.

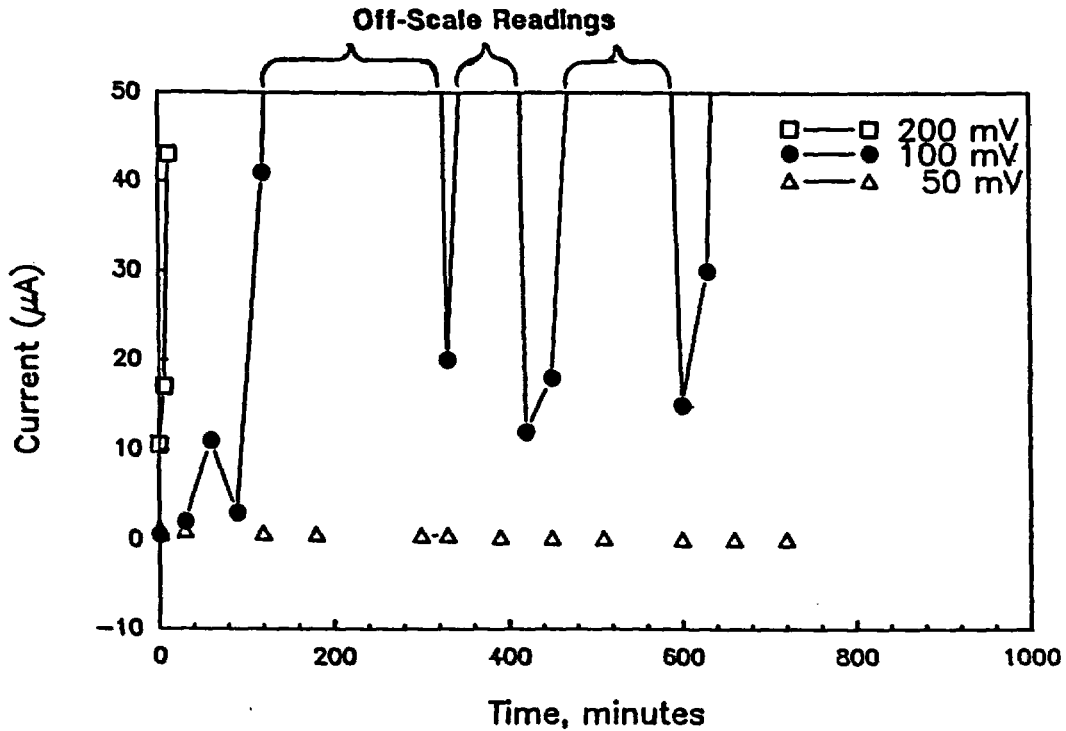


Figure 5-8. Current-Time Transients for Alloy G3 in Solution E4 Following Pit Stimulation at 0.6V (SCE) for 15 Seconds (0.25 min) and Polarized to a Potential Near  $E_{prot}$

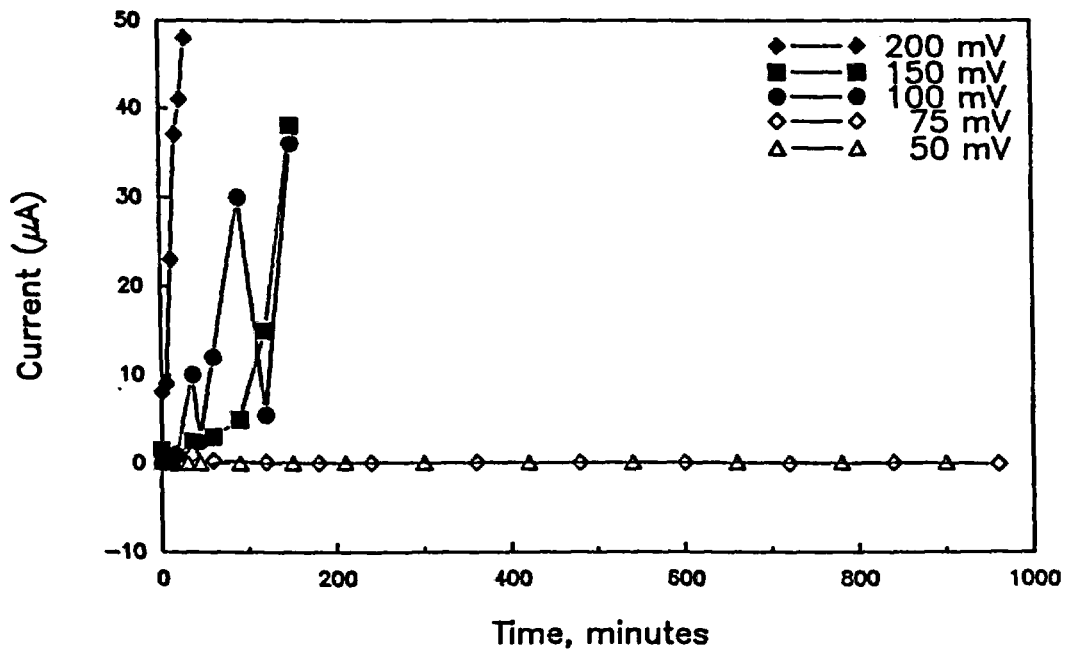


Figure 5-9. Current-Time Transients for Alloy G3 in Solution E4 Following Pit Stimulation at 0.6V (SCE) for 2 Minutes and Polarized to a Potential Near  $E_{prot}$

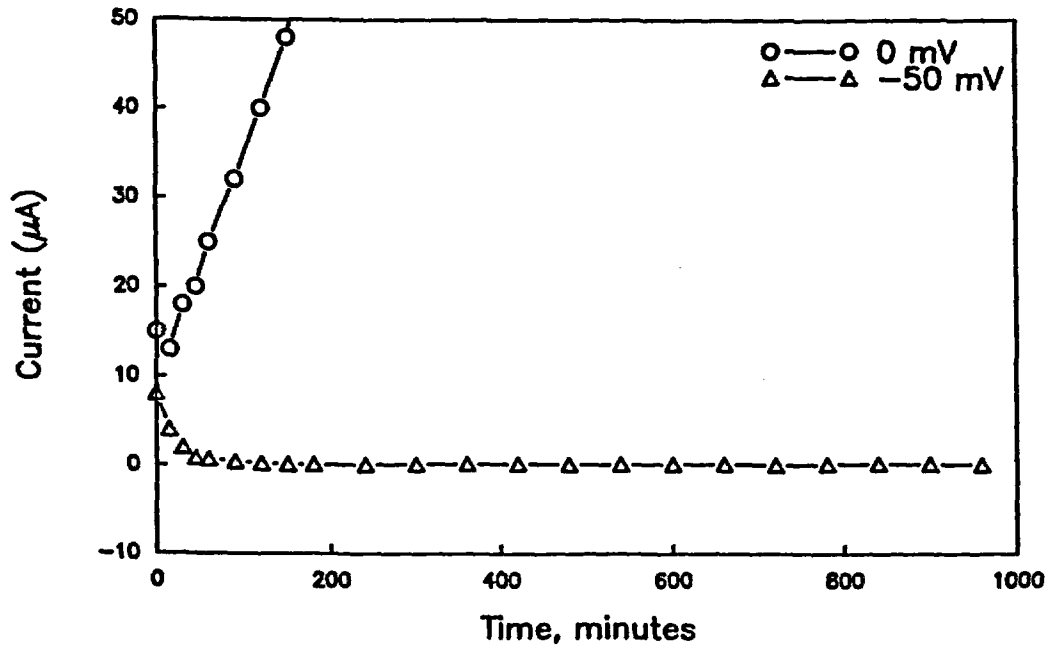


Figure 5-10. Current-Time Transients for Alloy G3 In Solution E4 Following Pit Stimulation at 0.6V (SCE) for 40 Minutes and Polarized to a Potential Near  $E_{prot}$

# 6

## DISCUSSION

There remains a great deal of controversy concerning the significance of  $E_{\text{pit}}$  and  $E_{\text{prot}}$ , the relationship between them, and the most appropriate method to measure them. In terms of the stochastic models that have been developed,<sup>1,2</sup>  $E_{\text{pit}}$  is expressed as the most active potential at which the frequency of pit nucleation exceeds zero. However, having a pit nucleation frequency greater than zero is not the only prerequisite for pit initiation. Another is an incubation period to allow the transition from an unstable to a stable pit.

The presence of preferred pitting sites, e.g., a specimen/holder interface or a second-phase inclusion on the free surface, is an additional factor that can affect the incubation time requirement. Therefore, preferred pitting sites can affect the value of  $E_{\text{pit}}$  measured by any method involving potential scanning, stepping, or holding a potential for a given time period. In the present study, this was most obvious in the CPP tests for Alloy G3 in Solution E4 in which pitting was observed in only one of three tests with a vapor/liquid interface present on the specimen; while pitting was observed in all three tests with a PTFE holder/specimen interface (pits preferentially initiated at the interface in two of the three tests). From the above discussion, it is clear that pit initiation has a significant dependence on potential, time, and specimen geometry and preparation.

$E_{\text{prot}}$  has typically been defined by other workers as the potential at which ongoing pits repassivate. Suzuki and Kitamura<sup>26</sup> described  $E_{\text{prot}}$  as the potential equal to the steady-state potential within the pit with no anodic

polarization applied. That is, repassivation occurs when the potential at the specimen surface is decreased to a value below that of the inside of the pit, thereby producing a net cathodic current within the pit. Therefore,  $E_{\text{prot}}$  would be dependent upon the environment within the pit which is, in part, controlled by the amount of pitting prior to its measurement (Wilde and Williams<sup>18</sup>), and which is directly related to the time of pit propagation prior to measurement of  $E_{\text{prot}}$ .

To examine the potential and time dependence for pit initiation and repassivation, the  $E_{\text{pit}}$  and  $E_{\text{prot}}$  data from the CPP tests, constant potential-time tests, and modified ASTM Standard F-746 tests were combined in potential versus time plots. First of all, the CPP tests were analyzed to extract time parameters that correspond to those in the constant potential-time tests and the modified ASTM F-746 tests. Time prior to pit initiation was selected as the time to scan from  $E_{\text{prot}}$  (as measured on the reverse scan) to  $E_{\text{pit}}$  during the forward scan. It is realized that the potential is varying during this period, so this value of time is not exactly equivalent to the time in constant potential-time tests, but a reasonable comparison can be made. Also from the CPP data, a time for pit growth is calculated as the time following pit breakdown (at  $E_{\text{pit}}$ ) to the time, during the reverse scan, at which repassivation occurs ( $E_{\text{prot}}$ ). This time can then be compared to the time of pit stimulation in the modified ASTM F-746 tests, with similar reservations as discussed above for pit initiation times. Table 6-1 presents these time data for the CPP tests for Alloys 317L and G3 in Solutions E3 and E4, respectively.



**Table 6-1**  
**CPP Test Data Including (I) Relationship Between  $E_{pit}$  and Time to Scan From  $E_{prot}$  to  $E_{pit}$ , and (II) Relationship Between  $E_{prot}$  and Time From Pit Initiation to Repassivation**

Specimen Type	Scan Rate V/h	Pitting Sites	$E_{pit}$		$E_{prot}$		
			Potential V (SCE)	Time <sup>(a)</sup> (min)	Potential V (SCE)	Time <sup>(b)</sup> (min)	
<b>Type 317L In Solution E3</b>							
PTFE Holder/Specimen	0.6	I, S	+0.68	70	-0.05	135	
PTFE Holder/Specimen	0.6	I, (S)	+0.78	90	-0.05	121	
PTFE Holder/Specimen	0.06	I, (S)	+0.82	760	-0.17	1,100	
PTFE Holder/Specimen	0.06	I, (S)	+0.34	320	-0.08	930	
Vapor/Liquid	0.6	S	+0.54	45	+0.02	116	
Vapor/Liquid	0.06	S	+0.84	860	-0.02	1,110	
<b>Alloy G3 In Solution E4</b>							
PTFE Holder/Specimen	0.6	I	+0.70(R)	112	0.00	78	
PTFE Holder/Specimen	0.06	S	+0.20	350	-0.14	350	
Vapor/Liquid	0.6	None	-	-	-	-	
Vapor/Liquid	0.06	None	-	-	-	-	
Vapor/Liquid	0.06	S	+0.59(R)	1,170	+0.13	470	

(a) Time prior to pit initiation.

(b) Time following pit initiation to pit repassivation.

R: Pitting initiated during reverse scan.

I: Pits initiated at PTFE holder/specimen interface.

S: Pits initiated on general surface away from any interface.

( ): Less favored pit initiation site.

Figures 6-1 and 6-2 show the potential versus time plots for Type 317L stainless steel in Solution E3 and for Alloy G3 in Solution E4, respectively. Data are presented for each of the three measurement techniques: CPP, constant potential-time, and modified ASTM F-746. For the

constant potential-time tests, each  $E_{pit}$  data point corresponds to the time prior to pit initiation at the test potential; a data point with an arrow indicates that no pit initiation occurred in that particular test for the time period indicated.

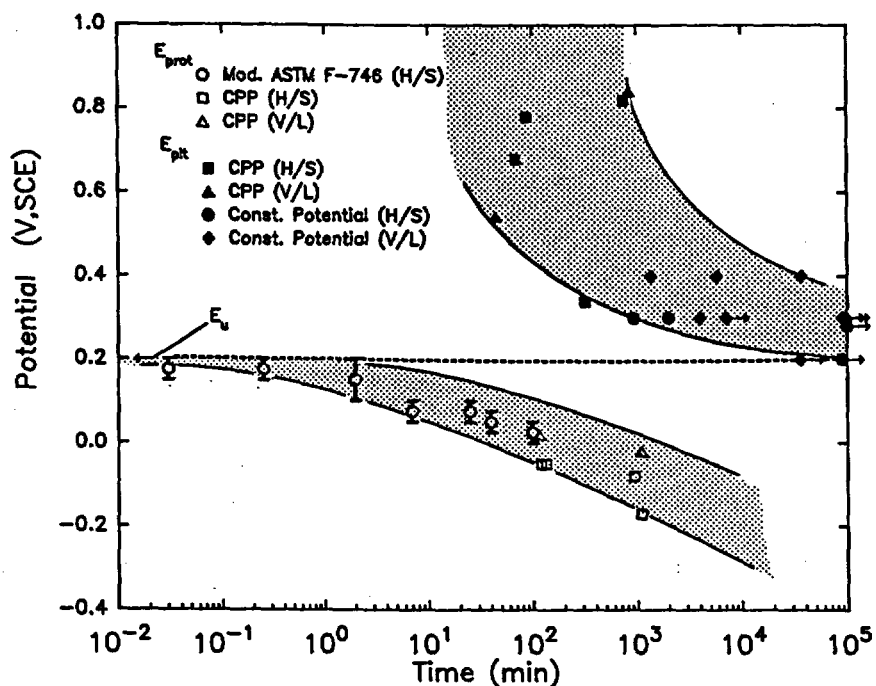


Figure 6-1. Potential Versus Time Data for Alloy 317L In Solution E3 for  $E_{pit}$  and  $E_{prot}$  ( $E_{pit}$  Versus Time to Pit Initiation and  $E_{prot}$  Versus Time Permitted to Pit)

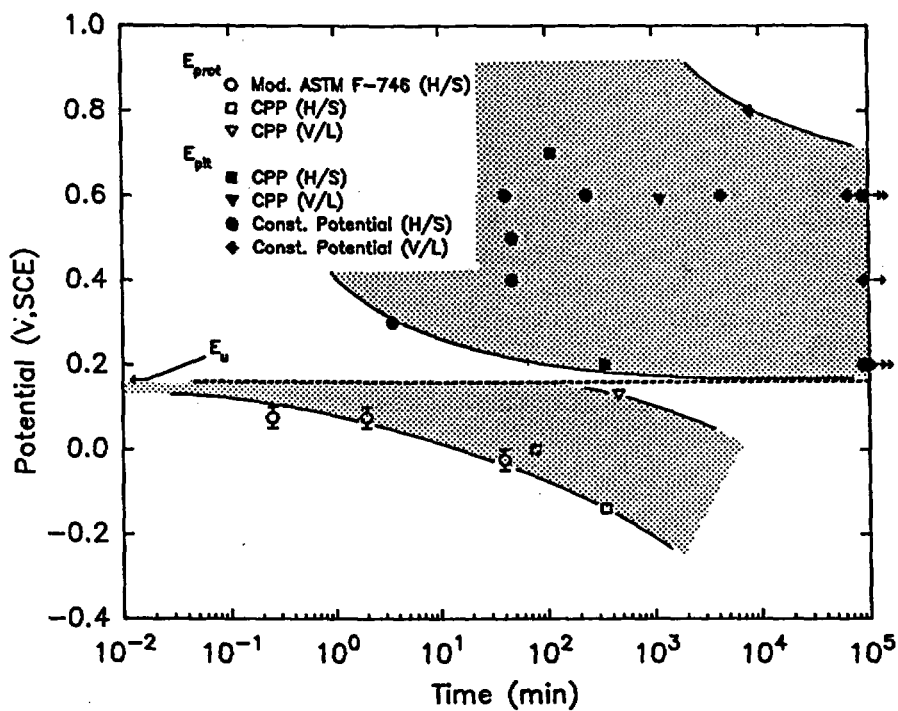


Figure 6-2. Potential Versus Time Data for Alloy G3 In Solution E4 for  $E_{pit}$  and  $E_{prot}$  ( $E_{pit}$  Versus Time to Pit Initiation and  $E_{prot}$  Versus Time Permitted to Pit)

There is significant scatter in the data for both alloy/solution combinations. The more important concept being considered is whether the most active value of  $E_{\text{pit}}$  equals the most noble value of  $E_{\text{prot}}$ , the latter being associated with repassivation of pits that have been permitted to grow only a minimal amount. The data in Figure 6-1 suggest that, for Type 317L stainless steel in a low-pH, high-chloride environment (10 g/L  $\text{Cl}^-$ ),  $E_{\text{prot}}$  and  $E_{\text{pit}}$  approach the same potential. For Type 317L, the difference between the most negative value of  $E_{\text{pit}}$  and the most positive value of  $E_{\text{prot}}$  is less than 100mV, possibly close to zero. For Alloy G3 (Figure 6-2), this difference is less than 70mV.

The suggestion that  $E_{\text{prot}}$  and  $E_{\text{pit}}$  approach a single value can be explained in terms of a conventional stochastic model of pitting. In this model, a unique  $E_{\text{pit}}$  value is defined as the most active potential at which the pit nucleation frequency exceeds zero. A nucleation event is characterized by a local increase in (anodic) current density which, in the case of a nonpropagating pit, is transitory; but which, in the case of a stable pit nucleus, remains higher than the initial passive current density. At potentials more active than this unique pitting potential ( $E_u$ ) any tendency to initiate a pit in the bulk environment is overwhelmed by the tendency to repassivate it, so no new pits are initiated. This also satisfactorily describes  $E_{\text{prot}}$  if pit growth has been negligible. Therefore, in the special case of a pit that has been propagating for a very short period, the environment within the pit will be quite similar to the bulk environment and  $E_{\text{prot}}$  should have a similar value to  $E_u$ . To state this concept in another way (Equation 6-1), the most active  $E_{\text{pit}}$  value possible is equal to the potential at which the pit nucleation frequency approaches zero, which is also the most noble potential that growing pits can be repassivated.

$$E_{\text{pit}} = E_u = E_{\text{prot}} \quad (6-1)$$

Pits that have propagated some significant amount are more difficult to repassivate because the environment within the confines of the pit is more aggressive (higher in  $\text{Cl}^-$  and lower pH) than the bulk. Thus, in general,  $E_{\text{prot}}$  values measured after significant pitting will be lower than  $E_u$ .

The above analysis implies that  $E_{\text{pit}}$  values will draw ever closer to  $E_u$ , the slower the scan rate in CPP tests, the longer the exposure time allowed in constant potential tests, and when incubation times are minimized by the presence of preferred pitting sites (e.g., PTFE holder/specimen interface). In addition, these "long-term" values of  $E_{\text{pit}}$  should be similar to the values of  $E_{\text{prot}}$ , determined by such means as the modified ASTM Standard F-746 test, where only a minimal time for pit growth is allowed prior to repassivation.

In this study, significant scatter was observed in the  $E_{\text{pit}}$  values in the CPP data and in the incubation time for pit initiation at a constant potential. In a previous study for EPRI for the same alloys in similar solutions, the scatter observed in the CPP tests was not nearly as great.<sup>34</sup> It is speculated that this increased scatter in  $E_{\text{pit}}$  is due to achieving a "better" PTFE holder/specimen interface. By removing preferred pit initiation sites, pit initiation occurred at less preferred sites, which introduced a greater amount of variation. In the previous EPRI study,<sup>34</sup> no attempt was made to remove the PTFE holder/specimen interface as a preferred site for pit initiation, which resulted in more reproducible and consistently more negative  $E_{\text{pit}}$  values.

# 7

## CONCLUSIONS

---

Based on the literature review and the testing program, the following conclusions are drawn concerning electrochemical measurements for pitting susceptibility.

1. Pit initiation can be described by a unique pitting potential,  $E_u$ , which is approximately equal to (a) the most negative  $E_{pit}$  value recorded in CPP tests or constant potential tests (associated with slow scan rates or long incubation periods), and (b) the most positive  $E_{prot}$  value when prior pit growth is minimized.
2. CPP tests tend to separate  $E_{pit}$  and  $E_{prot}$  by minimizing incubation time and maximizing pit growth following pit initiation.
3.  $E_{prot}$  from the CPP test is more conservative (more negative) than  $E_u$  and is an acceptable basis for most engineering decisions.
4.  $E_{pit}$  is less conservative (more positive) than  $E_u$  and is not an acceptable basis for engineering decisions involving long-term pitting performance predictions.
5. Deliberate incorporation of preferential pit initiation sites in a CPP test specimen is desirable from an engineering viewpoint to minimize the effect of incubation time and maximize the chances of pit initiation during this relatively short-term test.

## REFERENCES

---

1. D.E. Williams, C. Westcott, and M. Fleischmann. "Stochastic Models of Pitting Corrosion of Stainless Steels, I." *Journal Electrochemical Society*, 132, 8, p. 1796 (1985).
2. D.E. Williams, C. Westcott, and M. Fleischmann. "Stochastic Models of Pitting Corrosion of Stainless Steels, II." *Journal Electrochemical Society*, 132, 8, p. 1804 (1985).
3. F. Zucchi, I.H. Omar, and G. Trabanelli. "Inhibition of Pitting Corrosion of AISI 304 by Organic Compounds." *Werkstoffe Und Korrosion*, 38, pp. 742-745 (1987).
4. R.K. Dayal, N. Parvathavarthini, and J.B. Gnana-moorthy. "A Study of Various Critical Pitting Potentials for Type 316 Stainless Steel in Sulfuric Acid Containing Chloride Ions." *Corrosion*, 36, 8, pp. 433-436 (1980).
5. P.E. Manning, D.J. Duquette, and W.F. Savage. "The Effect of Test Method and Surface Condition on Pitting Potential of Single- and Duplex-Phase 304L Stainless Steel." *Corrosion*, 35, 4, 151-157 (1979).
6. P.E. Manning and D.J. Duquette. "The Effect of Temperature on Pit Initiation in Single-Phase and Duplex 304L Stainless Steels in 100ppm Cl Solution." *Corrosion Science*, 20, pp. 597-610 (1980).
7. "Relative Critical Potentials for Pitting Corrosion of 304 Stainless Steel, Incoloy 800, and Inconel 600 in Alkaline High-Temperature Aqueous Solutions." *Journal of Nuclear Materials*, 115, pp. 339-342 (1983).
8. M. Urquidi and D.D. Macdonald. "Solute-Vacancy Interaction Model and the Effect of Minor Alloy Elements on the Initiation of Pitting Corrosion." *Journal of Electrochemical Society*, 132, 3, pp. 555-558 (1985).
9. W.R. Clesiak and D.J. Duquette. "An Electrochemical Study of Pit Initiation Resistance of Ferritic Stainless Steels." *Journal of Electrochemical Society*, 132, 3, pp. 533-537 (1985).
10. R. Fratesi. "Statistical Estimate of the Pitting Potential of AISI 316L Stainless Steel in 3.5% NaCl Measured by Means of Two Electrochemical Methods." *Corrosion*, 41, 2, pp. 114-117 (1985).
11. D.M. Aylor and P.J. Moran. "A Comparison of Electrochemical Techniques for Assessing the Pitting Behavior of Aluminum Alloys in Seawater." Paper No. 216, *Corrosion 85*, National Association of Corrosion Engineers (1985).
12. J. Nader-Roux, A.M. de Becdelievre, G. Bouyssoux R. Roux, and J. de Becdelievre. "Study of Pitting Potential and Repassivation of Austenitic Steel in Chloride Medium." *Metaux-Corros-Ind.*, 60, 716, pp. 111-116 (1985).
13. N. Nilsen and E. Bardal. "Short Duration Tests and a New Criterion for Characterization of Pitting Resistance of Aluminum Alloys." *Corrosion Science*, 17, pp. 635-646 (1977).

## References

14. N. Azzzerri, F. Mancia, and A. Tamba. "Electrochemical Prediction of Corrosion Behavior of Stainless Steels in Chloride Containing Water." *Corrosion Science*, 22, 7, pp. 675-687 (1982).
15. J.L. Dawson and M.G.S.Ferreira. "Crevice Corrosion on 316 Stainless Steel in 3% NaCl Solution." *Corrosion Science*, 26, 12, pp. 1027-1040 (1986).
16. D.M. Aylor and P.J. Moran. "The Influence of Incubation Time on the Passive Film Breakdown of Aluminum Alloys in Seawater." *Journal of Electrochemical Society*, 133, 5, pp. 868-872 (1986).
17. B.C. Syrett. "PPR Curves—A New Method of Assessing Pitting Corrosion Resistance." *Corrosion*, 33, 6, pp. 221-224 (1977).
18. B.E. Wilde and E. Williams *Electrochemical Acta*. 16, p. 1971 (1971).
19. D.E. Williams and C. Westcott. "Proceedings of the 9th International Conference on Metallic Corrosion, Toronto, 1984." Vol. 4, p. 390, National Research Council of Canada, Ottawa, Ontario, Canada (1984).
20. G. Daufin, J. Pagetti, J.P. Labbe, and F. Michael. "Pitting Initiation on Stainless Steels: Electrochemical and Micrographic Aspect." *Corrosion*, 41, 9, pp. 533-539 (1985).
21. A. Broli and H. Holtan. "Determination of Characteristic Pitting Potentials for Aluminum by Use of the Potentiostatic Methods." *Corrosion Science*, 17, pp. 59-69 (1977).
22. B.C. Syrett, R. Viswanathan, S.S. Wing, and J.E. Wittig. "Effect of Microstructure on Pitting and Corrosion Fatigue on 17-4 pH Turbine Blade Steel in Chloride Environments." *Corrosion*, 38, 5, pp. 273-282 (1982).
23. Y. Ishikawa and H.S. Isaacs. "Study of Pitting Corrosion on Aluminum by Means of The Scanning Vibrating-Electrode Technique." Mechanical Engineering Research Laboratory Technical Report, B & L-33059, DE83-013065 (1983).
24. J.L. Dawson and M.G.S. Ferreira. "Electrochemical Studies of the Pitting of Austenitic Stainless Steel." *Corrosion Science*, 26, 12, pp. 1009-1026 (1986).
25. G. Okamoto, K. Tachibana, S. Nishiyama, and T. Sugita. "The Analysis of Passive Current Noise on Stainless Steels Under Potentiostatic Conditions With and Without Chloride Ions." *Passivity and Its Breakdown of Iron Base Alloys*, National Association of Corrosion Engineers, Houston, TX, pp. 106-109 (1973).
26. T. Suzuki and Y. Kitamura. "Testing Method for Localized Corrosion of Stainless Steel Considering the Corrosion Potential in its Environment." In *Proceedings of the Fifth International Congress on Metallic Corrosion*, Tokyo, Japan, NACE, pp. 1070-1073 (1972).
27. S.T. Hirozawa. "Determination of the Protection (Pitting) Potential by the Zap-Galvanostaircase Method." Paper No. 270, *Corrosion/86*.
28. A. Viebeck and D.W. DeBerry *Journal of Electrochemical Society*, Volume 131, p. 1844 (1984).
29. D.W. DeBerry and A. Viebeck, , *Journal of Electrochemical Society*, Volume 133, p. 32, 1986).
30. D.W. DeBerry and A. Viebeck. "Inhibition of Pitting Corrosion of Type 304L Stainless Steel by Surface Active Compounds." Paper No. 196, *Corrosion/86*.
31. S.T. Hirozawa. "Galvanostaircase Polarization: A Powerful Technique for the Investigation of Localized Corrosion." Paper No. 48 at the Electrochemical Society Meeting, Detroit, MI, October, 1982.
32. T.R. Beck. "Experimental Observations and Analysis of Hydrodynamic Effects on Growth of Small Pits." Interim Technical Report, March/78-February/79, N00014-76-C-0495 (1979).
33. K. Sugimoto, S. Matsuda, Y. Ogiwara, and K. Kitamura "Microscopic Ellipsometric Observation of Change in Passive Film on 18Cr-8Ni Stainless Steel with the Initiation and Growth of Pit." *Journal of Electrochemical Society*, 132, 8, pp. 1791-1995 (1985).
34. G.H. Koch, N.G. Thompson, and J.M. Spangler. "The Effects of SO<sub>2</sub> Scrubber Environments on Alloy Corrosion." EPRI report CS-4697, Electric Power Research Institute, Palo Alto, CA (1986).

